



HAL
open science

Tuning structure and properties of pectin aerogels

Sophie Groult, Tatiana Budtova

► **To cite this version:**

Sophie Groult, Tatiana Budtova. Tuning structure and properties of pectin aerogels. European Polymer Journal, 2018, 108, pp.250-261. 10.1016/j.eurpolymj.2018.08.048 . hal-02419292

HAL Id: hal-02419292

<https://hal.science/hal-02419292v1>

Submitted on 20 Mar 2023

HAL is a multi-disciplinary open access archive for the deposit and dissemination of scientific research documents, whether they are published or not. The documents may come from teaching and research institutions in France or abroad, or from public or private research centers.

L'archive ouverte pluridisciplinaire **HAL**, est destinée au dépôt et à la diffusion de documents scientifiques de niveau recherche, publiés ou non, émanant des établissements d'enseignement et de recherche français ou étrangers, des laboratoires publics ou privés.

Tuning structure and properties of pectin aerogels

Sophie Groult, Tatiana Budtova*

MINES ParisTech, PSL Research University, Center for Materials Forming (CEMEF),

UMR CNRS 7635, CS 10207, 06904 Sophia Antipolis, France

Corresponding author: Tatiana Budtova

[email: Tatiana.budtova@mines-paristech.fr](mailto:Tatiana.budtova@mines-paristech.fr)

tel : +33 4 93 95 74 70

Sophie Groult: Sophie.groult@mines-paristech.fr

Abstract

Highly porous and nanostructured pectin aerogels were synthesized via dissolution-solvent exchange-drying with supercritical CO₂. **The goal was to show why and how aerogel morphology and properties vary as a function of external conditions.** Polymer concentration, pH and concentration of mono- and divalent metal salts were varied. The way of structure stabilization, i.e. gelation or direct non-solvent induced phase separation (in other words, the state of the matter before solvent exchange, gel or solution) turned out to be one of the key parameters influencing aerogel morphology and density. When strong gels were formed via calcium-induced gelation at pH around pK_a, the corresponding aerogels presented large pores, the lowest density (0.04 – 0.05 g/cm³) and lowest specific surface area (around 270 - 350 m²/g). On the contrary, when pectin network was formed via non-solvent induced phase separation from non-gelled pectin solutions during solvent exchange step, the resulting aerogels were mesoporous, with highest density (0.12 – 0.15 g/cm³) and highest specific surface area (around 600 m²/g). The results obtained provide the guidelines for making aerogel matrices with fully controlled morphology and properties.

Keywords

Pectin; Solutions; Gels; Aerogels; Structure-properties correlations

Highlights

- Pectin aerogels of various densities and surface areas were synthesized
- The mechanism of structure formation, gelation or phase separation, is the key in structure control
- Correlations between polymer ionization, pH, presence of ions and aerogel properties are built

1. Introduction

Aerogels are highly porous and lightweight nanostructured materials composed of a solid network with air in the pores. Aerogels are usually obtained from a gel in which the liquid phase is replaced by air. In order to prevent the collapse of network structure during drying due to capillary forces, drying in supercritical (sc) conditions is performed. Classical aerogels based on silica, synthetic polymers and their carbons typically possess low density ($< 0.2 \text{ g/cm}^3$), open pores in the range of small macro- and mesopores and very high specific surface area (700 - 1500 m^2/g) [1]. These structural properties make aerogels attractive materials for a broad variety of applications such as thermal and acoustic insulation, catalyst support, fuel cells, capacitors, absorption and adsorption, flame retardancy, ultrasound probes and ion exchange media.

Bio-aerogels are new versatile materials based on polysaccharides. The latter are widely available, renewable, non-toxic, biocompatible and can be easily functionalized due to a large amount of hydroxyl groups on polymer backbone. Bio-aerogels are thus suitable for a wide range of life science applications such as biomedical, pharmaceutical, biotechnological, cosmetic and food. For example, bio-aerogels were suggested to be used as biodegradable solid matrices for pharma and biomedical applications: as drug delivery systems [2–7] and as 3D cellular scaffolds [8–11] for tissue engineering.

The requirements towards aerogel chemical, mechanical and structural properties are dictated by the application. Thus the understanding of how formulation and external conditions (polymer ionization and concentration, solution pH, presence of ions, etc) influence aerogel properties is a key issue. For instance, recently we showed how to tune pectin aerogel structure to reach thermal super-insulation properties, *i.e.* with conductivity being below that of air [12]. The latter required, on one hand, a compromise between material low density, which provides low heat conduction via solid phase, and on the other hand, small

pore sizes, decreasing the conduction via gaseous phase. In order to use aerogel as biocompatible drug carriers, drug loading and release kinetics are critical parameters to consider regarding the therapeutic indications [13]. By tuning aerogel matrix chemical and physical properties, the drug dose and release into physiological fluids can be varied in a wide range of release kinetics, from immediate release (for example, hydrophilic silica aerogel) [14,15] to delayed release (gastro-resistant materials, for example, pectin hydrogels) [16] or extended release (for example, nanofibrillated cellulose aerogels) [17]. Finally, for 3D cell scaffolds, bio-compatibility, mechanical stability, open porosity and certain pore size are critical factors to ensure cell viability, growth and differentiation. In particular, pore size distribution and connectivity have to be precisely set to regulate cell adhesion and mobility within the material: for cell attachment pores should be below one micron, for cell–cell interactions - around micrometric scale (a few microns) and for cell functioning pores should be large, around a few hundreds of microns [18,19].

Despite the importance of morphology control, very little is known about the correlations between the type of polysaccharide, processing conditions and aerogel structure and properties. In this work we used pectin extracted from citrus, a ramified polysaccharide with gelling abilities, to produce pectin based aerogels, also called “aeropectins”. Pectin was selected because it allows numerous variations of conditions that influence solution viscosity and gelation. **As it will be demonstrated, this allows obtaining wide range of aerogel morphologies and properties. Moreover, pectin has gastro-resistant properties which open prospects in using pectin aerogels in oral drug delivery applications.** Pectin is a polyelectrolyte composed of a linear chain of galacturonic acids units (Gal.A), branched with ramosyl units and neutral sugars. Carboxylic acids of Gal.A can be methyl-esterified defining a degree of esterification (DE). Depending on the DE, pectins are generally classified as Low Methylated (LM, DE < 50%) or High Methylated (HM, DE > 50%). In aqueous

media the gelation of pectin solutions depends on temperature, pectin concentration, presence of co-solutes, pH, ionic strength and concentration of metal ions. Acid functions of non-methylated Gal.A are likely to be dissociated into carboxylates at pH higher than pK_a (3-3.5). Depending on polymer concentration, physical gelation may occur in acidic conditions ($pH < 3.5$) at room temperature. In this case, pectin network is mainly formed by chain entanglements stabilized by hydrogen bonds involving hydroxyl and protonated carboxyl groups and hydrophobic interactions between methyl-ester groups [20,21]. At pH close or above pK_a the addition of divalent cations, such as calcium, leads to another gelation mechanism involving the formation of intermolecular junction zones via ionic bonds following the “egg-box” model [22]. In this case, the dissociated acid groups of non-methylated Gal.A units interact with divalent cations and create strong intermolecular ionic bridges. Ionic gelation is predominant for LM pectin gels due to a higher proportion of non-methylated Gal.A as compared to HM pectins.

In the present study, pectin aerogels were obtained by polymer dissolution in water, exchange of water to a fluid miscible with CO_2 and supercritical drying with CO_2 . While our previous work was focused only on the correlations between pectin aerogel thermal conductivity and morphology [12], the present investigation provides wide and detailed overview on how and why aerogel structure and properties vary as a function of external conditions. The latter are studied in a systematic way by varying pectin concentration, solution pH, type and concentration of metal salts ($CaCl_2$ and $NaCl$) and nature of non-solvent. The role of solution gelation or not, and of the mechanisms of network formation in aerogel precursor are suggested and discussed. This study demonstrates the ways of controlling structure formation in pectin-based aerogels, and presumably, in other gelling polyelectrolyte polysaccharides such as alginates and carrageenans. Emphasis is made on the

multiscale correlations between the properties of dissolved polymer, mechanisms of network formation and the final structure and properties of pectin aerogels.

2. Experimental

2.1. Materials

Citrus pectin with the degree of esterification 35% (as given by the provider) was kindly donated by Cargill. Calcium chloride anhydrous powder (96% extra pure) from Acros Organics was used to make CaCl₂ aqueous solutions. Sodium chloride salt (99.5%, analysis grade) was from Acros Organics. Ethanol (purity > 99%, laboratory reagent grade), acetone (> 99%, laboratory reagent grade), potassium hydroxide pellets (extra pure), hydrochloric acid (32%, analysis grade, certified analytical reagent) were from Fisher Scientific and used as received. Water was distilled.

2.2. Methods

2.2.1. Preparation of pectin aerogels

Pectin aerogels were prepared as described previously, via dissolution – gelation (in some cases gelation did not occur) – solvent exchange – drying with sc CO₂ [12]. Pectin aqueous solutions were prepared by dissolution of pectin powder in distilled water at 65 °C under stirring at 400 rpm [12]. Pectin concentrations are given in weight percent (wt %) unless otherwise mentioned. After complete dissolution, solution pH was adjusted^[1] by addition of small quantity of HCl or KOH. pH was varied from 0.5 to 5. Pectin solutions were then poured into molds of 27.5 mm of diameter, in certain cases sodium (NaCl) or calcium solution

^[1] Some degradation may be possible at very low and high pH due to acid hydrolysis or β -depolymerization and demethoxylation in neutral to alkaline conditions [23–25]. This resulted in aerogel poor mechanical properties, especially at pH 0.5, and texture deterioration, as it will be shown in Results section.

(CaCl₂) was added under stirring. The molar ratio R of metal cation (Me), Na⁺ or Ca²⁺, to pectin carboxyl groups, expressed in mol.L⁻¹, was varied from 0.05 to 2 and calculated as follows:

$$R = \frac{[Me]}{[RCOO^-]} \quad (1)$$

It was not possible to prepare homogeneous calcium-containing gels (from CaCl₂) at pH > 3 due to immediate ionic gelation leading to highly heterogeneous samples.

Pectin solutions were let at rest for 48 h at room temperature. Depending on the conditions (concentration, pH, presence of CaCl₂ or NaCl) solutions were gelling or not as determined by a simple “tilting test” (solution flowing or not); the state of solution will be given for each aerogel studied.

In order to perform drying with sc CO₂, water has to be replaced by a fluid which is miscible with CO₂. Two kinds were used; ethanol and acetone, both are pectin non-solvents. Solvent exchange was performed by progressively decreasing water/non-solvent (v/v) ratio to 50/50, 25/75 and 0/100, followed by the final extensive washing with pure non-solvent. The resulting aerogel precursor was 3D network composed of coagulated pectin with non-solvent in the pores. The precursors were then dried with sc CO₂ (see details on drying parameters in Ref. [12, 26]).

The final dimensions of dried samples were disks with diameter around 15-25 mm and thickness around 6-10 mm depending on sample shrinkage which in turn is controlled by pectin concentration and state of matter before solvent exchange (solution or gel), presence of CaCl₂, *etc.*, see photos of pectin aerogels in Figure 1.

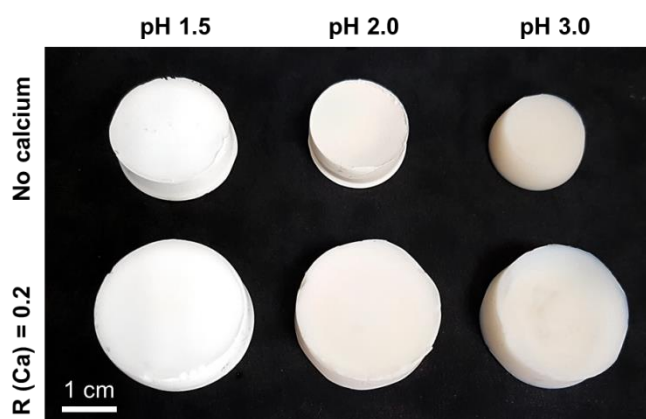


Figure 1

Photos of pectin aerogels from 3 wt% solutions prepared in different conditions at pH 1.5, pH 2.0 and 3.0, without the addition of salts and with addition of calcium at $R(\text{Ca}) = 0.2$. Without calcium at pH 1.5 the sample before solvent exchange was weak acid gel, at pH 2.0 it was high viscosity solution and at pH 3.0 low viscosity solutions. At $R(\text{Ca}) = 0.2$ strong ionic gels were obtained at all pH. Non-solvent was ethanol.

2.2.2. Viscometry

Viscometry was used to determine pectin molecular weight. Pectin was dissolved in 0.01 M NaCl, and dilution was performed at 26.6 °C according to Ref. [27]. iVisc from LAUDA and capillary Ubbelohde Dilution Viscometer Type I with capillary diameter 0.63 mm was used to determine pectin intrinsic viscosities using Huggins approach.

2.2.3. Rheology

The rheological measurements were performed on Gemini rotational rheometer with Peltier temperature control system, using cone-plate geometry, both of 60 mm of diameter and cone with an angle of 2°. Solutions were let at rest for 1 h at room temperature prior the analysis. A pre-shear at 20 s⁻¹ was applied for 120 s before performing rheological measurements.

Steady state viscosity as a function of shear rate was measured with increasing shear rate from 0.1 to 600 s⁻¹ for 0.9 % pectin solutions at 20 °C and various pH. In these conditions solutions are not gelling.

2.2.4. Sample shrinkage and aerogel density and porosity

Volume shrinkage ΔV of samples was determined before drying (*i.e.* at the end of solvent exchange) and after sc drying:

$$\text{Volume shrinkage, \%} = \frac{V_0 - V_i}{V_0} \times 100 \% \quad (2)$$

where V_0 is the volume of the gel before solvent exchange and V_n is sample volume at the corresponding step.

Bulk density ρ_{bulk} was determined as the ratio of sample mass to volume. The mass of the aerogel was measured with digital analytical balance with a precision of 0.01 mg. The volume was measured with digital caliper.

Porosity was calculated as follows:

$$P, \% = 1 - \frac{\rho_{bulk}}{\rho_{skeletal}} \quad (3)$$

where $\rho_{skeletal}$ is 1.5 g/cm³ [12].

Pore specific volume was estimated using bulk and skeletal densities:

$$V_{pores} = \frac{1}{\rho_{bulk}} - \frac{1}{\rho_{skeletal}} \quad (4)$$

2.2.5. Specific surface area

Specific surface area (S_{BET}) was determined by nitrogen adsorption using Micromeritics ASAP 2020 and BET method. Prior to analysis, samples were degassed in a high vacuum at 70 °C for 10 h.

It should be noted that it is not possible to experimentally measure total pore volume and pore size distribution using nitrogen adsorption: pore volume obtained with BJH approach gives only about 10-15% of the total pore volume [12,28,29]. Mercury porosimetry does not

allow measuring pore volume of pectin aerogels either, and, in general, of most of bio-aerogels': samples are compressed and thus pore volume "measured" is an artefact [29,30].

2.2.6. Scanning electron microscopy

Scanning electron microscopy (SEM) observations of aerogels morphology were performed on a Supra40 Zeiss SEM FEG (Field Emission Gun) at a voltage of 3 KeV. Prior to observations, a fine layer of about 7 nm of platinum was sputtered onto the sample surface with metallizer Q150T Quarum.

3. Results

Pectin is a polyelectrolyte, and thus the changes of solution pH and/or addition of ions influence solution viscosity and may induce gelation. Gelation mechanism, in turn, depends on the type of the external parameter. This is well known and described in literature. The open question is how pH and ions' concentration influence pectin aerogel morphology and properties. The following sections are structured as follows. After determination of pectin molecular weight, the Results section describes the effect of pectin concentration, solution pH, and concentrations of calcium and sodium ions on aerogel morphology and properties, keeping one parameter varied and the other constant. Finally, the Discussion section summarizes all findings and makes general suggestions on the influence of external parameters and state of the matter, solution or gel, on pectin aerogel properties.

3.1. Determination of pectin molecular weight

Huggins method was used to determine pectin intrinsic viscosity $[\eta]$ in 0.01 M NaCl at 26.6 °C. These conditions were used as far as they allow the calculation of pectin molecular weight according to Mark-Houwink equation:

$$[\eta] = KM^a \quad (3)$$

where $K = 0.0234$ and $a = 0.8221$ [27]. The dependence of reduced viscosity on pectin concentration is shown in Figure S1 of the Supplementary Information. The intrinsic viscosity of pectin in these conditions is 339 mL/g and molecular weight is $1.15 \cdot 10^5$ g/mol.

3.2. Influence of non-solvent type and pectin concentration on aerogel structure and properties

To study the influence of non-solvent type, acetone vs ethanol, and of pectin concentration on pectin aerogel properties, several batches of pectin solutions from 2 to 8 wt% at pH 3 were prepared. pH 3 was selected because pK_a is around 3–3.5 for low methylated pectins [31,32].

Sample volume shrinkage was monitored before and after sc drying (see Figure S2 of the Supplementary Information). At the end of solvent exchange the shrinkage is around 10 - 20 vol%, with highest shrinkage for 2% solution (40 vol%), and it is similar for both non-solvents. The overall shrinkage after drying is around 50 – 80 %, it is slightly higher for ethanol. Shrinkage decreases with the increase of pectin concentration. This phenomenon had already been reported for other bio-aerogels: higher polymer concentration makes the network more “resistant” to sample contraction [33,34].

Figures 2a and 2b present pectin aerogel density and specific surface area as a function of pectin concentration and type of non-solvent at pH 3. The use of acetone resulted in lower density and higher specific surface area. For example, for the initial solutions of 3 wt%, aerogel density was around 0.11 g/cm^3 and specific surface around $570 \text{ m}^2/\text{g}$ when using ethanol as the non-solvent, whereas while using acetone density was 0.065 g/cm^3 and specific surface reached the values up to $630 \text{ m}^2/\text{g}$. Similar phenomena were recorded for aerogel made at pH 2 (Figure S3 of the Supplementary Information). Some works suggest that the larger the difference in Hansen solubility parameters between the polymer and non-solvent, the higher is sample shrinkage [35,36]. However, pectin is heteroglycan and Hansen

parameter(s) are not known. It may be possible that the miscibility of non-solvent and CO₂ also plays a role: acetone is better miscible with CO₂ than ethanol according to Hansen solubility parameters (of ethanol it is 26.5 MPa^{1/2}, of acetone 19.9 MPa^{1/2} and of CO₂ 17.4 MPa^{1/2}) [37]. In all the cases studied density of pectin aerogels was from two (for acetone) to more than three (for ethanol) times higher than that of the theoretical no-shrinkage case (Figure 2a). As expected, density increases with the increase of polymer concentration in solution.

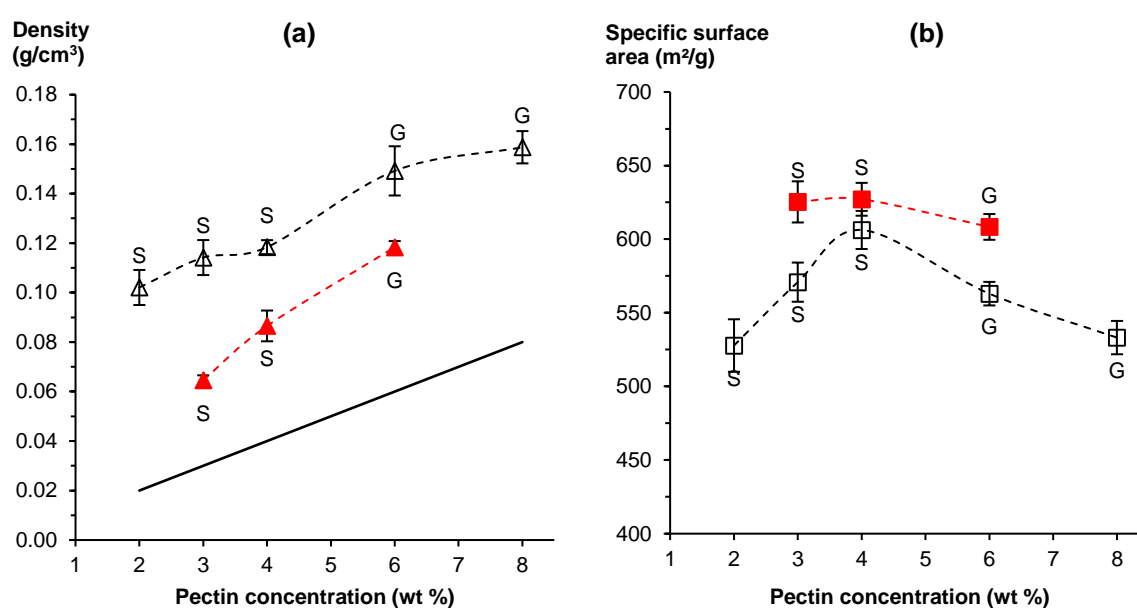


Figure 2

Density (a) and specific surface area (b) as a function of pectin concentration for solvent exchange performed in ethanol (open points) and acetone (filled points). Pectin was dissolved at pH 3.0, the state of the matter before solvent exchange, solution (S) or gel (G), is indicated for each case. Solid line is theoretical density for no-shrinkage case; dashed lines are given to guide the eye.

It is difficult to conclude now on the influence of concentration on specific surface area. The reason is that at pH 3, pectin dissolved at 2, 3 and 4 % is solution, and at 6 and 8 % it is

gel. Previous studies on cellulose aerogels [33,38] reported the increase of specific surface area with the increase of polymer concentration which is also the case for pectin aerogels made from 2, 3 and 4 % solutions. The result for cellulose aerogels was interpreted by the decrease of pore size and not increase of pore wall thickness with the increase of polymer concentration [33]. In the case of cellulose the state of the matter before solvent exchange was the same thought all experiments: it was a solution for cellulose dissolved in ionic liquid and in NaOH-urea-water [33,38]. As it will be shown later, the state of the matter before solvent exchange strongly influences pectin shrinkage and thus aerogel density and morphology.

Pectin aerogel porosity and pore volume of the same samples as shown in Figure 2 are shown in Figure S4 of the Supplementary Information. All values are lower for aerogels prepared with ethanol as non-solvent as compared to those prepared with acetone, which is expected from the values of density and specific surface area. The increase of pectin concentration leads to the decrease in porosity and pore volume for both types of non-solvents used. Pore volume varies from 5.6 to 9.1 cm³/g for aerogels made with ethanol as non-solvent and it is 30 to 80 % higher for acetone case.

SEM images of pectin aerogel morphology are presented in Figure 3, for two pectin concentrations and two non-solvents. Solvent exchange with acetone resulted in slightly larger pores with less agglomerated pore walls compared to ethanol. The increase of pectin concentration makes the network denser and with smaller pores. The thickness of pore walls is around 7 to 14 nm as estimated from Figure 3, with some rare chain agglomerates/packages from around 20 to 30 nm of thickness, see an example on Figure S5 of the Supplementary Information. Average fibril size D can also be roughly calculated as $D = 4/(\rho_{\text{bulk}}S_{\text{BET}})$ assuming that fibrils are ideal rods of uniform thickness and the same skeletal density. With S_{BET} varying from 530 to 630 m²/g, D is around 4 to 5 nm, which fits well the experimental observations after subtracting from the latter few nanometers of sputtered platinum.

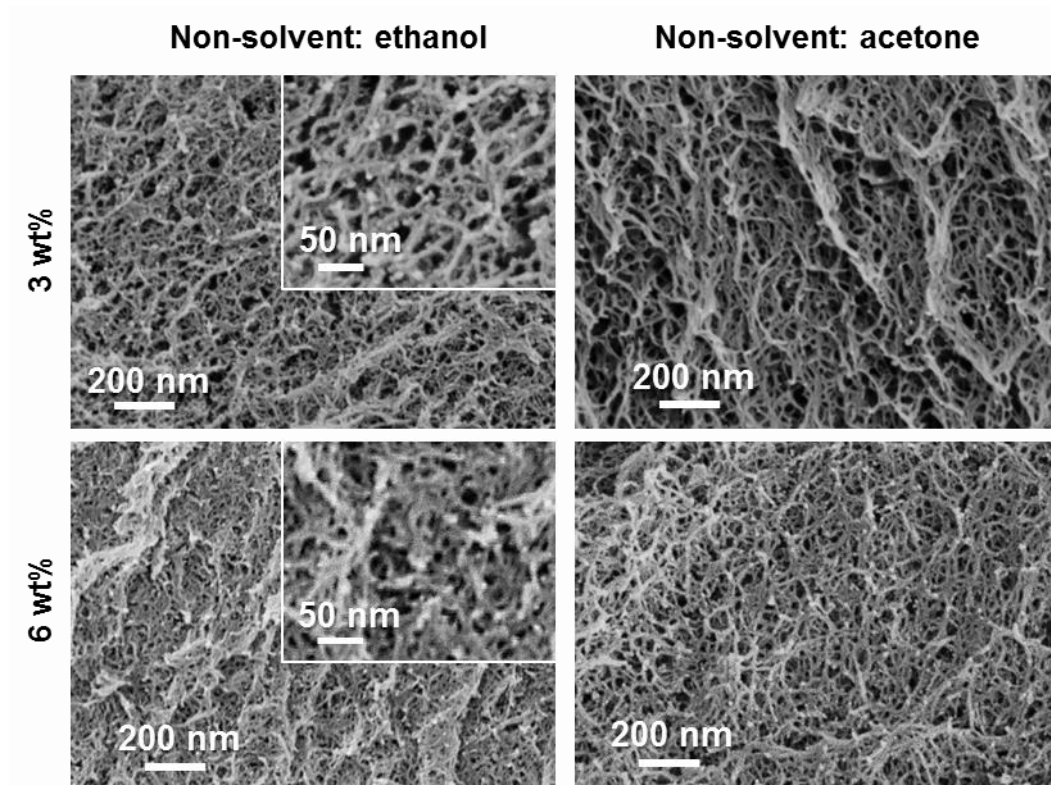


Figure 3

SEM images of pectin aerogels made from 3 wt% and 6 wt% pectin solutions at pH 3, with ethanol (a) or acetone (b) as non-solvent.

3.3. Influence of pH on aerogel structure and properties

It is known that dissolved pectin, being a polyelectrolyte, is very sensitive to pH. At low pH chains associate and are stabilized by hydrogen bonding between un-dissociated free carboxylic acids and secondary alcohol groups, and by hydrophobic interactions between methyl esters [20]. This is reflected by change of solution viscosity at lower polymer concentration, and may lead to so-called acid gelation if the number of junction zones is sufficient, the latter depending on solution temperature and pectin concentration [39–41].

To better understand the influence of pH on pectin aerogel structure and properties, we illustrate the effect of pH on pectin chains' interactions via viscosity η of semi-dilute pectin

solutions (0.9 wt%) as a function of shear rate $\dot{\gamma}$ at different pH (Figure 4). At pH below $pK_a \approx 3$, solutions showed a strong shear-thinning behavior, and viscosity increases with decreasing pH due to macromolecules association. This is especially pronounced at pH below 2.5 when ionization of pectin chains is significantly reduced. At higher pectin concentrations and below pH 2 solutions may form a gel. The increase of pH above pK_a leads to progressive deprotonation of carboxylic acids into carboxylates. The coulombic repulsion and high hydration of pectin macromolecules prevent polymer aggregation [42]. Beyond pH 4 practically no evolution of viscosity as a function of pH was observed, as ionization of carboxylates is supposed to be complete. In this case, pectin solutions exhibit stable and low viscosity as each polysaccharide chain is hydrated, extended and independent [42].

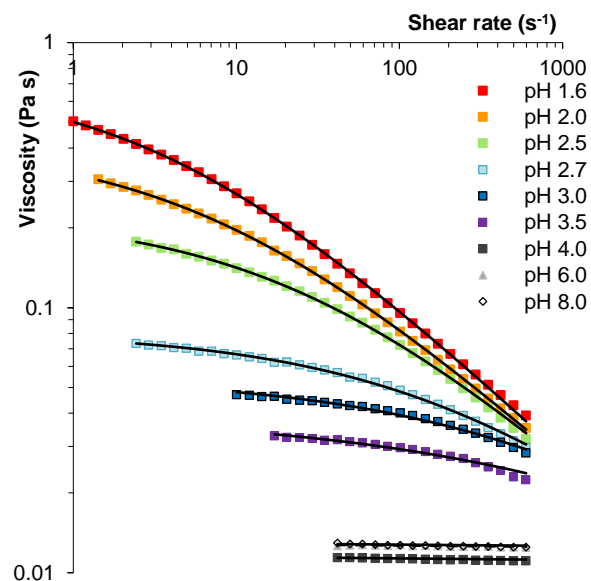


Figure 4

Viscosity as a function of shear rate of 0.9 wt% pectin solutions at different pH at 20 °C.

Solid lines correspond to viscosity approximated with Cross model.

The flow curves were fitted using simplified Cross model:

$$\frac{\eta(\dot{\gamma})}{\eta_0} = \frac{1}{1+(\alpha \cdot \dot{\gamma})^n} \quad (4)$$

where η_0 is zero shear rate viscosity, α is constant and n is flow index (or Cross exponent).

The fitting parameters are presented in Table S1 of the Supplementary Information. Zero shear rate viscosity and flow index as a function of pH are shown in Figure 5. These results confirm what was qualitatively deduced from Figure 4: a strong drop of zero shear rate viscosity and of flow index with the increase of pH and the independence of these parameters on pH at pH > 4.

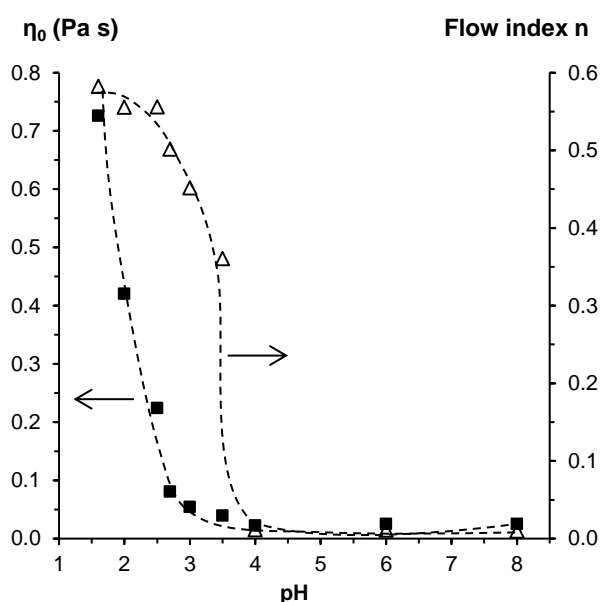


Figure 5

Zero shear rate viscosity (squares) and flow index (triangles) (see eq.4) of 0.9 wt% pectin solutions as a function of pH at 20 °C. Dashes lines are given to guide the eye.

Pectin aerogels were made from 3 wt% solutions at various pH. Acid-induced gels were obtained at room temperature and pH of 0.5, 1.0, 1.5 and pH 1.8. At higher pH solutions were not gelling and aerogel precursors were obtained by direct solvent exchange with ethanol. In this case, viscosity of pectin solutions had to be sufficiently high for not deformed 3D

network to be formed; for example, it was not possible to obtain homogenous aerogels from solutions at $\text{pH} > 5$.

Figure 6a shows the shrinkage of pectin samples after solvent exchange and after drying and Figure 6b corresponds to density and specific surface area of the obtained pectin aerogels. A very interesting trend was obtained: all parameters show a convex shape as a function of pH, with the highest values of density and specific surface area almost tripled in the maximum.

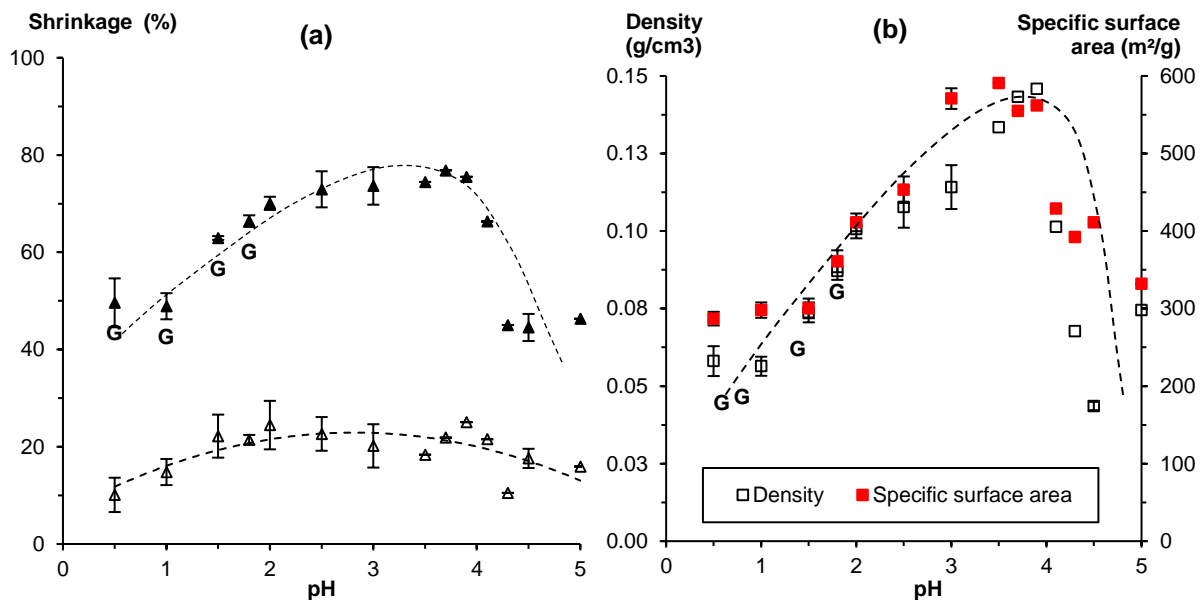


Figure 6

Influence of pH on (a) volumetric shrinkage after solvent exchange (open points) and after sc-drying (filled points) and (b) density (open points) and specific surface area (filled points) of pectin aerogels made from 3 wt% solutions. The state of the matter before solvent exchange is noted “G” for gel, the rest are solutions. Non-solvent used was ethanol. Dashed lines are given to guide the eye.

Shrinkage is around 10 – 20 vol% after solvent exchange and it strongly increases after sc-drying, especially for non-gelled solutions at $\text{pH} > 2$. The lower pH, the stronger pectin

network [43], providing better mechanical resistance to solvent exchange and drying. Gel state prevents shrinkage and preserves gel porous structure resulting in lower density and lower specific surface area (Figure 6b). Pectin aerogels at pH 0.5, 1 and 1.5 display large pores and thick pore walls (Figure 7). Porosity is around 95 – 96 % and pore volume around 13 – 17 cm³/g (Figure S5 in the Supplementary Information). It should be noted that at very low pH (pH ≤ 1) pectin acid degradation may have occurred as reported in Ref. [25], resulting in partly damaged morphology as observed by SEM (Figure 7).

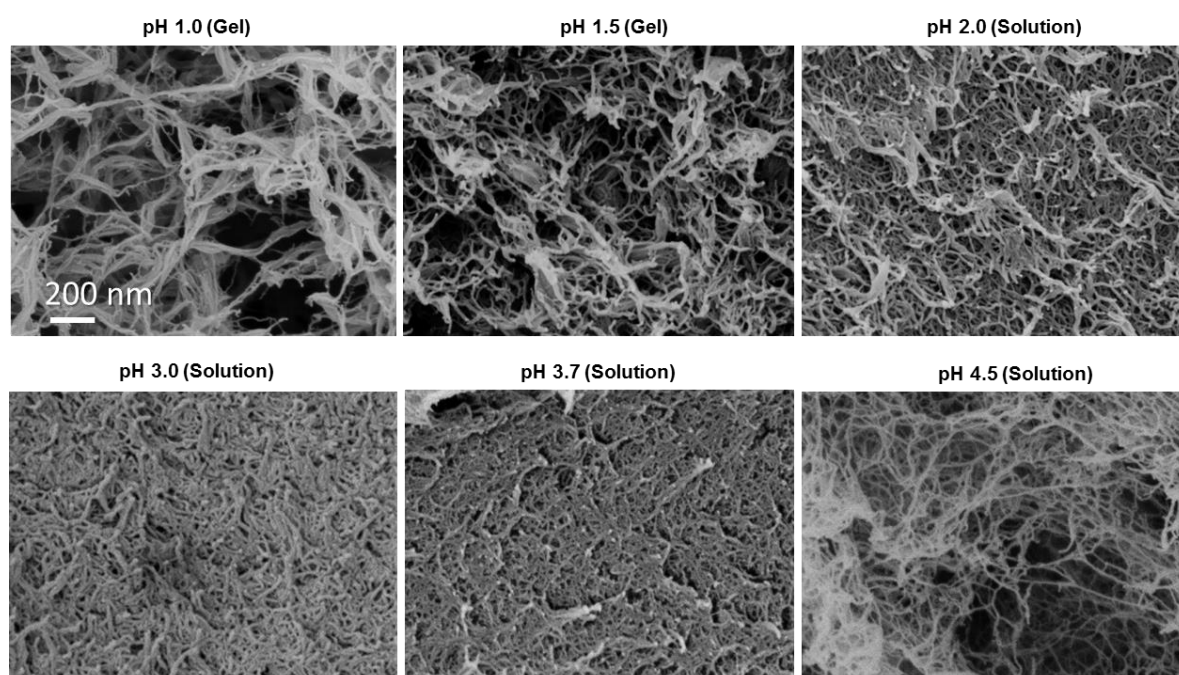


Figure 7

SEM images of pectin aerogel morphology made from 3 wt% solutions at different pH. The state of the matter before solvent exchange is indicated for each case. Non-solvent used was ethanol. The scale is the same for all SEM images.

With the increase of pH from 1.8 to 3 – 3.5, progressive ionization of pectin chains occurred decreasing the probability of their association, and gelation was inhibited. This induced high sample shrinkage, up to 75 vol% (Figure 6a), resulting in the increase of pectin aerogel density (Figure 6b). As a consequence, aerogel porosity and pore volume decreased to

90% and $6 \text{ cm}^3/\text{g}$, respectively (Figure S5 in the Supplementary Information). High shrinkage led to denser morphology and decrease of pore size (Figure 7): for example, pore size varied from 50 – 300 nm at pH 1 to much more homogeneous sizes around 30 – 50 nm at pH 3 as estimated from SEM images. Because at pH 3 – 3.5 aerogel density still remained low and pore size decreased as compared to pH 1 - 2, specific surface area strongly increased as pH increased, from around $300 \text{ m}^2/\text{g}$ at pH 1.5 to almost $600 \text{ m}^2/\text{g}$ at pH 3. We assume that at pH 3 – 3.5 due to the repulsion between charged chains their agglomeration was inhibited which led to higher specific surface area. Finally, due to complete pectin ionization at pH above 4, viscosities of pectin solutions were too low to lead to monolithic non-damaged samples during solvent exchange. After sc drying, pectin aerogels appeared to have very heterogeneous morphology, as can be seen in Figure 7, with lower mean bulk density and specific surface as compared to pH 3 – 3.5.

3.4. Effect of calcium ions on pectin aerogel structure and properties

The addition of divalent cations strongly impacts pectin gelation mechanism and thus potentially allows the variation of aerogel properties [44,45]. The ionized groups of non-methylated galacturonic acid on pectin backbone can create ionic bonds with divalent cations such as calcium [45,46]. Successive ionic bonds can form junction zones between unbranched non-esterified galacturonan segments of two pectin chains in a twofold helical conformation, retaining calcium ions in between, as described by the so-called “egg-box model” [22]. The ionic bonding results from specific non-covalent electrostatic interactions between free divalent cations and the oxygen atoms of the hydroxyl groups, the oxygen atoms of the glucosidic ring and the bridging oxygen atoms of dissociated galacturonic acids through their free-electron pairs [46]. These ionic junctions are stable when at least 7 to 20 successive ionic bonds are involved [47,48]. The cross-linking formed by ionic bonds between carboxylates

function and divalent cations such as calcium produce strong, brittle and less elastic pectin gels than those formed by hydrogen and hydrophobic interactions in acidic condition [49].

In order to understand the influence of calcium ions on the morphology and properties of pectin aerogels, we varied calcium concentration (or the molar ratio of calcium to pectin, $R(\text{Ca})$) at fixed pectin concentration 3 wt% and pH 3 which is pK_a of LM pectin. The photos of the obtained pectin aerogels with increasing $R(\text{Ca})$ ratio are given in Figure S7 of the Supplementary Information.

The addition of even low amount of calcium increases pectin solution viscosity; at $R(\text{Ca}) = 0.1$ a weak gel and at $R(\text{Ca}) \geq 0.2$ strong gels are formed. The influence of $R(\text{Ca})$ on samples' volumetric shrinkage is shown in Figure 8a and on aerogel density and specific surface area in Figure 8b. Shrinkage of pectin samples decreases with the increase of $R(\text{Ca})$, as calcium reinforces the network by the formation of large amount of strong ionic junction zones [50–53]. As a result, density of aerogels strongly decreases from 0.11 g/cm^3 without calcium to more than twice lower value, around 0.05 g/cm^3 , for $R(\text{Ca})$ above 0.2 (Figure 8b). Consequently, porosity and pore volume increase with the increase of calcium concentration (Figure S8 in the Supplementary Information).

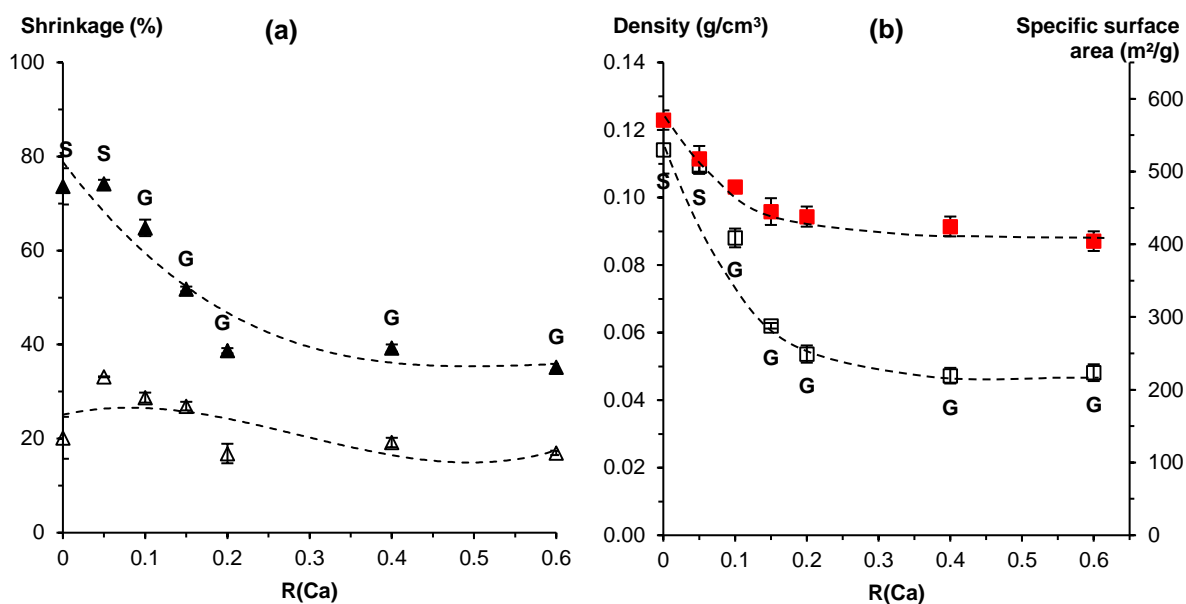


Figure 8

Influence of calcium to pectin molar ratio $R(\text{Ca})$ on (a) shrinkage after solvent-exchange (open points) and after sc drying (filled points) and (b) density (open points) and specific surface area (filled points) of pectin aerogels made from 3 wt% solutions at pH 3, non-solvent was ethanol. The state of the matter before solvent exchange, solution (S) or gel (G), is indicated for each case. Lines are given to guide the eye.

Specific surface areas of pectin aerogels decreased from around 600 to around 400 m^2/g with $R(\text{Ca})$ increase from 0 to 0.2, respectively (Figure 8b). The same trend for shrinkage, density and specific surface area was also found at pH 2 (Figure S9 in the Supplementary Material). It has to be noted that at pH 2 the addition of calcium had a smaller impact on pectin aerogel properties as far as carboxyl deprotonation of galacturonic groups is lower at pH 2 than at pH 3 [54].

The addition of calcium has a strong impact on pectin aerogel morphology, as shown on the representative SEM images in Figure 9. The higher the $R(\text{Ca})$, the stronger the gels with

less shrinkage and larger pores, from around 30-50 nm without calcium to 100 - 150 nm at $R(\text{Ca}) > 0.2$. Similarly to acid gelation by lowering pH (see Section 3.3), calcium induced gelation leads to better preservation of network morphology and of macropores, as observed by SEM. Beyond $R(\text{Ca}) = 0.2$, the morphology of aerogels is quite similar, except that very fast gelation at $R(\text{Ca}) > 0.4$ led to heterogeneities due to unevenly dispersed calcium ions. The reason is that the maximum amount of calcium possible to be bound to pectin is around stoichiometric ratio, 0.3 to 0.6 depending on pectin degree of methylation [45,55,56], which corresponds to molar ratio $R(\text{Ca})$ from 0.15 to 0.3 as obtained above.

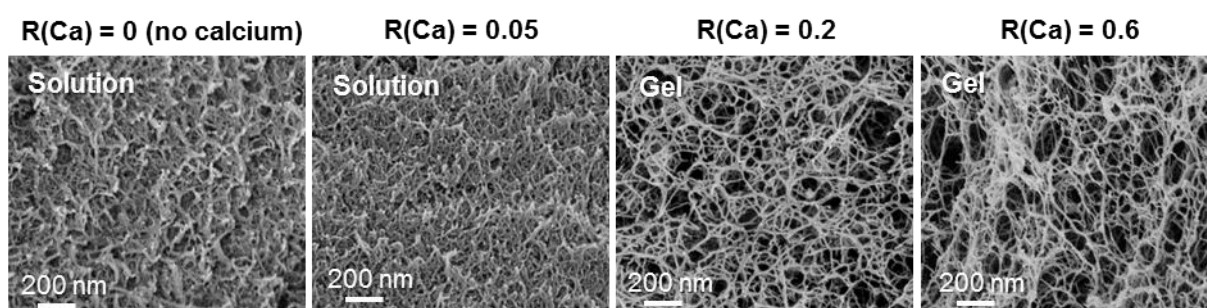


Figure 9

SEM images of pectin aerogels made from 3 wt% solutions at pH 3 with calcium chloride at $R(\text{Ca}) = 0.05, 0.2$ and 0.6 . The scale is the same for all images. The state of the matter before solvent exchange is indicated for each case. Non-solvent used was ethanol.

3.4. Effect of monovalent ions (NaCl) on pectin aerogel structure and properties

Monovalent metal ions also influence pectin solution viscosity and may induce solution gelation [57–59]. Although ions as sodium cannot create ionic bonds with pectin, they decrease electrostatic repulsions between dissociated carboxyl groups by screening [58,60]. This allows chains approaching each other and promotes hydrogen bonding and hydrophobic interactions potentially leading to a sort of acid-induced gelation [58]. Here we demonstrate the impact of the presence of sodium ions on pectin aerogel properties and morphology (see

photos of aerogels in Figure S10 in the Supplementary Information). The molar ratio of sodium to pectin $R(\text{Na})$ was varied from 0 to 2; at $R(\text{Na}) \geq 1$ (NaCl concentration 0.1 M) strong turbid gels were obtained.

Figure 10a shows samples' shrinkage as a function of sodium to pectin molar ratio for solutions of 3 wt% at pH 3. As for the case of the addition of calcium (Figure 8a), the presence of sodium ions resulted in lower shrinkage due to solution gelation. As a consequence, the increase in sodium concentration led to pectin aerogel lower density, from of $0.114 \pm 0.007 \text{ g/cm}^3$ at $R(\text{Na}) = 0$ to $0.069 \pm 0.001 \text{ g/cm}^3$ at $R(\text{Na}) = 2$ (Figure 10b), higher porosity and pore volume (Figure S11 in the Supplementary Information). Specific surface area (Figure 10b) decreased with the increase of $R(\text{Na})$, also as in the case of the addition of calcium. Similar trends were recorded for pectin aerogels made from higher pectin concentration, 6 wt% (Figure S12).

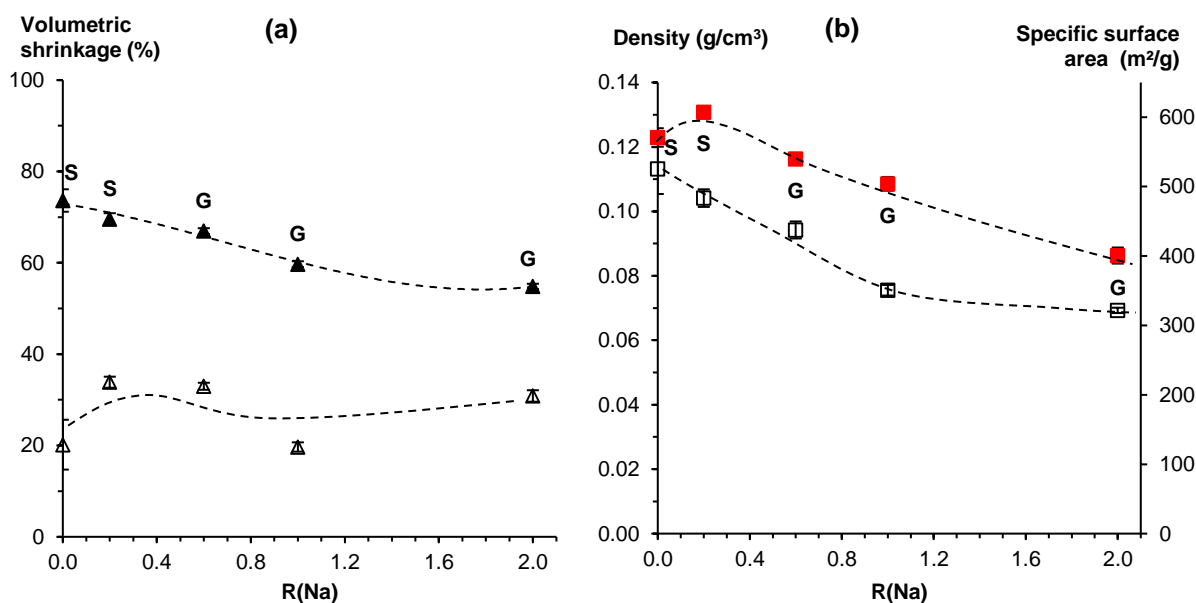


Figure 10

Influence of sodium to pectin molar ratio $R(\text{Na})$ on (a) shrinkage after solvent exchange (open points) and after drying (filled points) and (b) density (open points) and specific surface area (filled points) of pectin aerogels made from 3 wt% solutions at pH 3, non-solvent was ethanol.

The state of the matter before solvent exchange, solution (S) or gel (G), is indicated for each case. Lines are given to guide the eye.

The morphology of pectin aerogels depends on sodium concentration, see Figure 11. Non-gelled aerogel, in the absence of sodium, has compact morphology with the majority of mesopores while at $R(\text{Na}) = 2$ the morphology is similar to that in the presence of calcium, with rather large macropores.

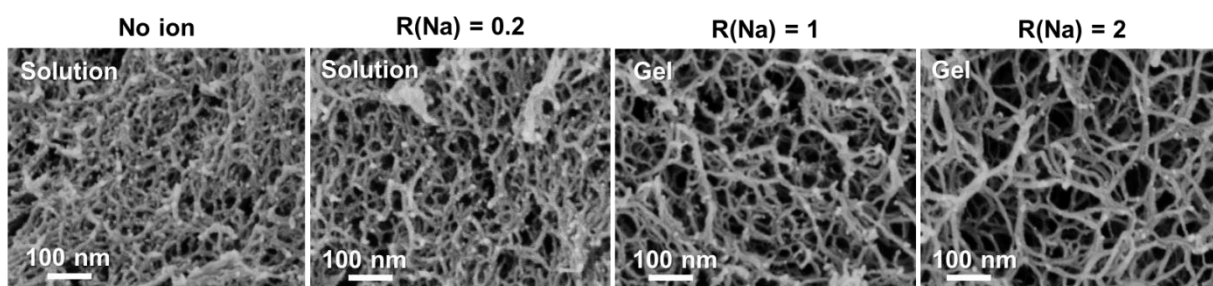


Figure 11

SEM images of pectin aerogels made from 3 wt% solutions at pH 3 with NaCl at $R(\text{Na}) = 0, 1$ and 2. The scale is the same for all images. The state of matter, solution or gel, is indicated for each case. Non-solvent was ethanol.

4. Discussion

The results presented above on the influence of pH and concentration of di- and monovalent metal ions on pectin aerogel morphology and properties show that the main factor governing aerogel characteristics is the mechanism of structure stabilization, or, in other words, the state of matter before solvent exchange, solution or gel. Gelation, whatever is the mechanism, leads to lower shrinkage upon the addition of non-solvent and sc drying and thus to aerogels with lower density and lower specific surface area, as macropores are preserved. When a non-solvent is added to non-gelled pectin solution, phase separation occurs (also

known as “immersion precipitation”) leading to a strong contraction of macromolecules. The particularity of polysaccharides is that above the overlap concentration coagulated pectin still forms porous 3D network structure. This network continues contracting during drying because of a huge difference in polarity of water-soluble pectin and highly apolar CO₂. Due to high volume shrinkage the density of aerogels increases (but still remains low, below 0.2 g/cm³) and specific surface area increases as macropores disappear.

An example of how pectin aerogel morphology and properties can be tuned by varying pH and calcium concentration is shown in Figure 10, where aerogel characteristics are modified with pH (below pK_a) and with calcium at R(Ca) = 0.2 (concentration 0.020 mM). Strong gels were obtained either by acid-induced gelation at pH < 1.5, or by ionic gelation with addition of calcium at pH close to pectin pK_a [43], both resulting in low-density pectin aerogels (≈ 0.05 g/cm³) with specific surface area around 300 – 450 m²/g. At pH close to pK_a ≈ 3 - 3.5 and without calcium, non-gelled pectin solutions consisting of dissociated chains were obtained, leading to aerogels with more than twice higher density (around 0.12 – 0.14 g/cm³) and high specific surface area (560 - 590 m²/g) as compared to low pH. The closer pH was to pK_a, the more significant was this difference between samples with or without calcium, gels vs solutions, respectively.

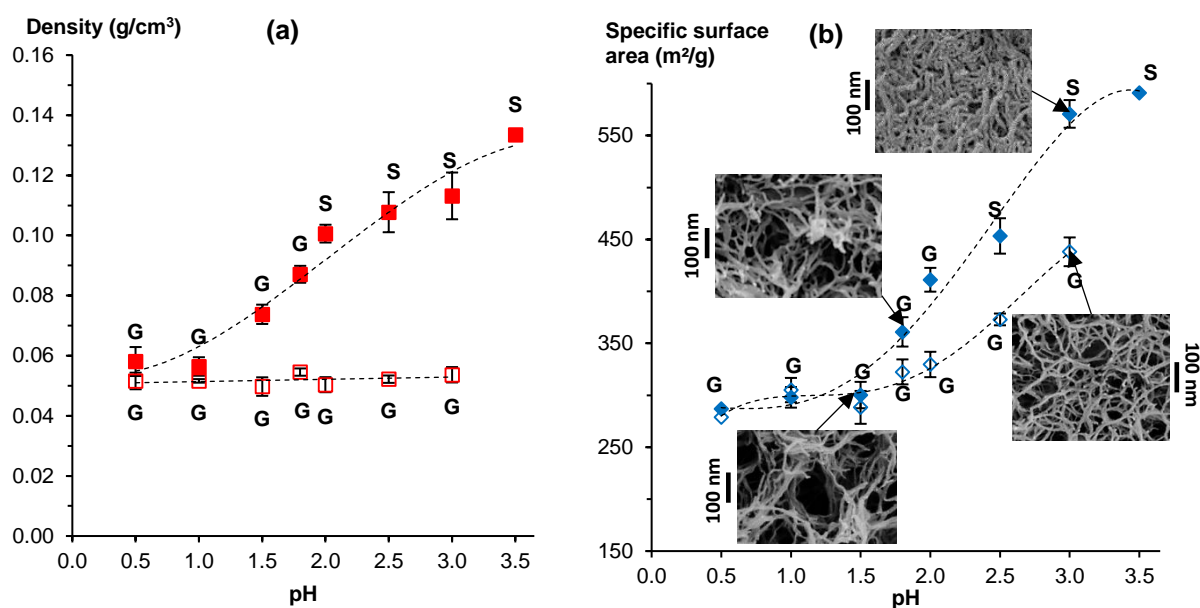


Figure 10

(a) Density and (b) specific surface area of pectin aerogels made from 3 wt% solution in absence (filled symbols) or with addition of calcium at $R(\text{Ca}) = 0.2$ (empty symbols) at different pH. At pH 3.5 gelation in the presence of calcium was too quick to obtain a homogeneous sample. The state of the matter before solvent exchange, solution (S) or gel (G), is indicated for each case. Dashed lines are given to guide the eye.

The second factor governing pectin aerogel morphology (less important than the state of matter but still noticeable) is the type of gelation mechanism, acid vs ionic gelation. Here we only compare aerogels obtained from gelled solutions. One example is shown in Figure 10 for the case $R(\text{Ca}) = 0.2$: at low pH gelation is mainly acid-induced and at pH around 3 it is ionic. At low pH pectin chains interact by assembling their non-dissociated galacturonic acid domains into intermolecular junction zones involving successive physical bonds. The latter are formed due to hydrogen and hydrophobic interactions. At low pH pectin ionization is very low, and thus acid-induced gelation is relatively unaffected by the addition of calcium. Because acid-induced gelation is a cooperative reaction, aerogel morphology is rather heterogeneous, with large pores and “blocks” of agglomerated chains (see SEM image in

Figure 10 at pH 1.5 and $R(\text{Ca}) = 0.2$). At pH around 3 – 3.5 ionic gelation occurs: aerogel density is the same as for acid-induced gelation (Figure 10a) but the morphology is much more homogeneous due to highly dissociated separated chains (see SEM image in Figure 10b at pH 3 and $R(\text{Ca}) = 0.2$). In this case specific surface area is higher than that at pH 1 – 1.5, 450 m^2/g vs 290 m^2/g , respectively, reflecting the larger fraction of mesopores which can also be seen on SEM images (Figure 10b).

Another example illustrating the influence of the type of gelation mechanism on aerogel morphology is shown in Figure 11 for the case of ionic (calcium-induced) vs acid (sodium induced) induced gelation. The first one results in ionic bonding between pectin chains [22], whereas the latter leads to screening of negative charges allowing acid gelation. The effect of the addition of sodium ions on gelation and pectin aerogel morphology and properties is similar to what was observed for calcium ions, but sodium cations had to be added in much higher concentration than calcium to influence the state of matter and aerogel properties. When calcium is added, strong gels are formed from 3 wt% solutions at very low ion concentration, $R(\text{Ca}) = 0.2$. On the contrary, at $R(\text{Na}) < 1$ weak gels are formed, resulting in higher density (Figure 11a) and higher specific surface area (Figure 11b); this case resembles non-gelled solutions. However, when $R(\text{Na})$ is ten times higher than calcium molar concentration, $R(\text{Na}) = 2$, acid gelation occurs leading to strong gels and aerogels with low density and rather low specific surface area, similar to those formed via ionic gelation.

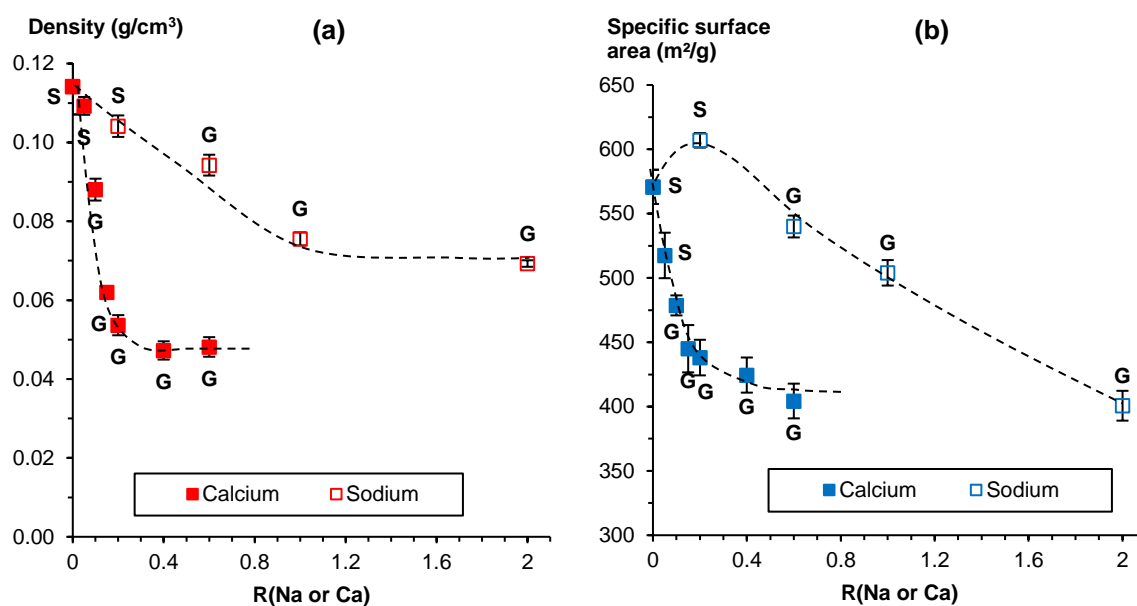


Figure 11

(a) Density and (b) specific surface area of pectin aerogels made from 3 wt% solutions pH 3.0 with either calcium (filled symbols) or sodium (open symbols), as a function of R molar ratio. The state of matter solution (“S”) or gel (“G”) is given for each case. Dashed lines are given to guide the eye.

The correlation between the state of the matter and aerogel density and specific surface area is summarized in Figure 12. Overall, density and specific surface area increase from roughly 0.05 g/cm³ and 300 m²/g to 0.15 g/cm³ and 600 m²/g, respectively, with the following evolution of the state of the matter before solvent exchange: strong gels → weak gels → high viscosity solutions → low viscosity solutions. Figure 12 shows results only for aerogels made from 3 wt% solution with non-solvent ethanol; the properties can be tuned even more if varying pectin concentration and non-solvent. A schematic presentation of structure evolution from pectin solution to aerogel, involving either gelation or phase separation, is shown in Figure 13. We hypothesize that this approach may be valid for other gelling polysaccharides such as carrageenans and alginate.

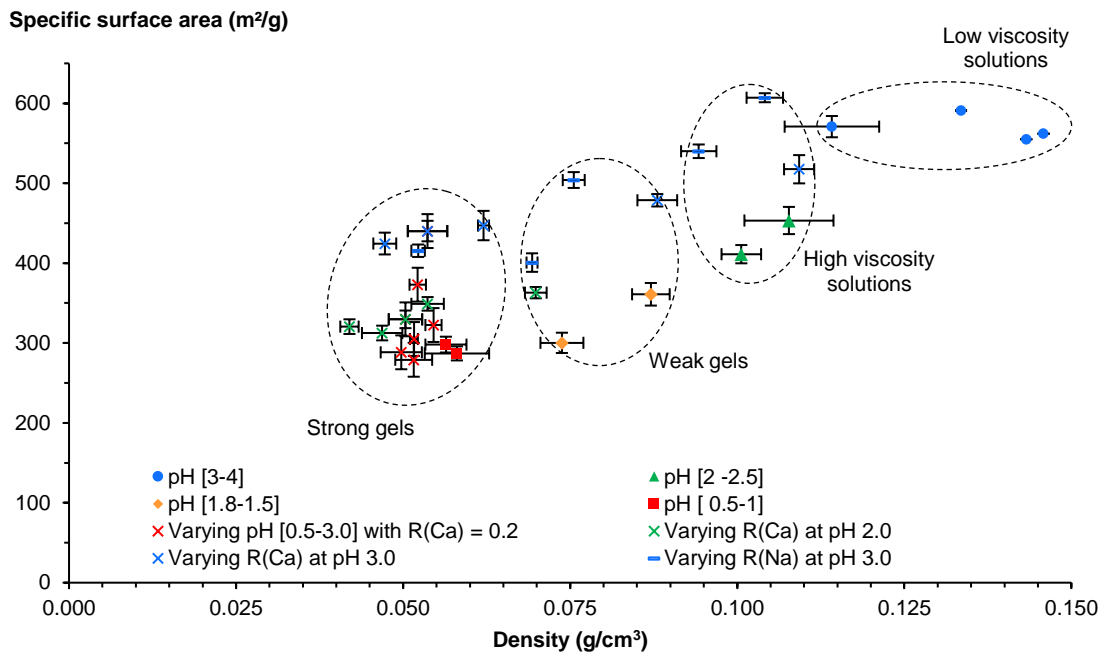


Figure 12

Density and specific surface area of pectin aerogel made from 3 wt% solutions, non-solvent is ethanol.

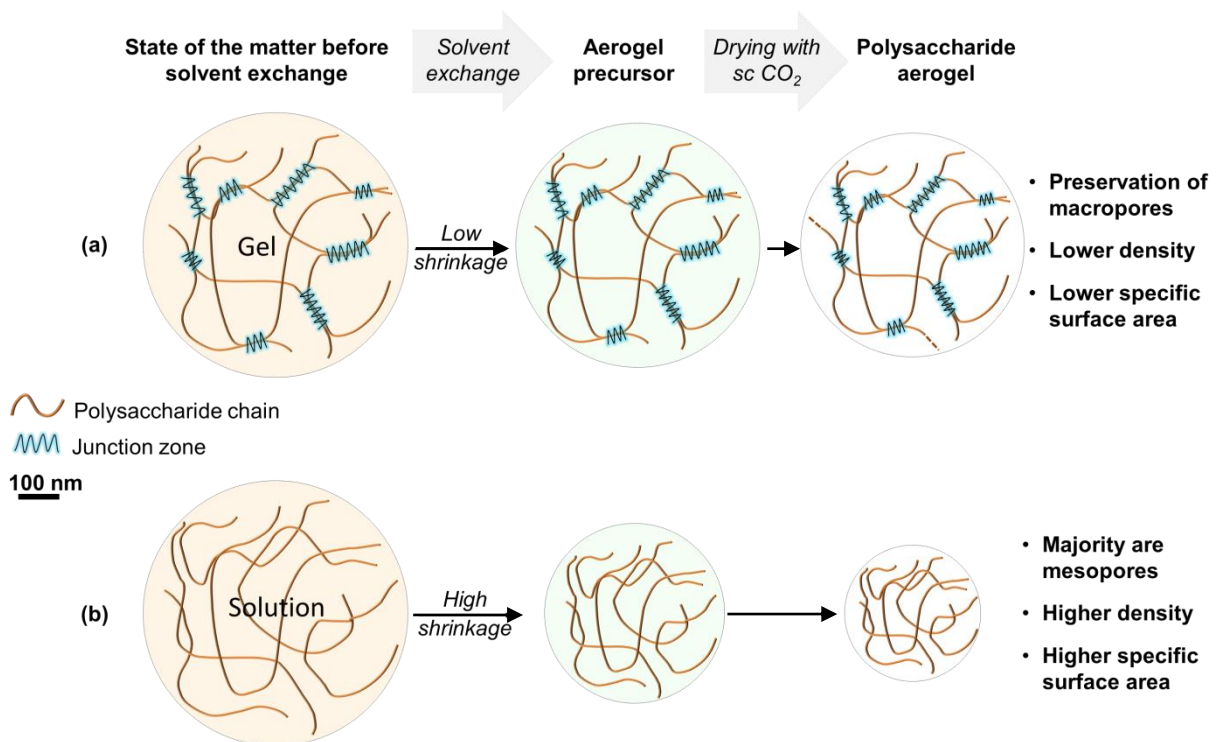


Figure 13

Schematic presentation of two main ways of structure formation, from solution to aerogel

5. Conclusions

Low methylated pectin aerogels were synthesized and characterized. A systematic variation of the external parameters (pH, polymer concentration, type of non-solvent, concentration of mono- and polyvalent metal ion salts) allowed modulating solution viscosity and gelation mechanisms, which in turn influenced aerogel structure and properties. The density of pectin aerogels varied from 0.05 to 0.15 g/cm³ and specific surface area from 270 to 600 m²/g.

Strong ionic gels formed in the presence of calcium around pectin pK_a “resisted” shrinkage during solvent exchange and drying. As a result, aerogels with high proportion of macropores, low density, around 0.05 g/cm³, and rather low specific surface area, around 300 m²/g, were formed. Aerogels with similar morphology and density were obtained at low pH: solutions gelled due to hydrogen bonding between protonated carboxyl groups and hydrophobic interactions between methylated groups. The increase of pH led to carboxylate groups’ ionization preventing gelation. The state of the matter before solvent exchange was solution and pectin network was formed during solvent exchange, via non-solvent induced phase separation (or coagulation). In this case shrinkage during solvent exchange and subsequent drying was high as far as 3D structure was not “stabilized”. The resulting pectin aerogels were mesoporous, of density around 0.12 -0.15 g/cm³ and high specific surface area, around 600 m²/g. Weak gels were formed upon the addition of sodium salt which was screening the electrostatic repulsion between charged carboxylates and leading to aerogels with properties intermediate to those described above. The mechanism of structure stabilization, *i.e.* gelation or non-solvent induced phase separation, was shown to be the key parameter controlling aerogel structure and properties.

Acknowledgements

Authors are grateful to Cargill for providing pectin. We thank Pierre Ilbizian (PERSEE, Mines ParisTech) for supercritical drying with CO₂.

References

- [1] M.A. Aegerter, N. Leventis, M.M. Koebel, eds., *Aerogels Handbook*, Springer New York, New York, NY, 2011. <http://link.springer.com/10.1007/978-1-4419-7589-8> (accessed January 4, 2016).
- [2] C.A. García-González, M. Jin, J. Gerth, C. Alvarez-Lorenzo, I. Smirnova, Polysaccharide-based aerogel microspheres for oral drug delivery, *Carbohydr. Polym.* 117 (2015) 797–806. doi:10.1016/j.carbpol.2014.10.045.
- [3] T. Mehling, I. Smirnova, U. Guenther, R.H.H. Neubert, Polysaccharide-based aerogels as drug carriers, *J. Non-Cryst. Solids.* 355 (2009) 2472–2479. doi:10.1016/j.jnoncrysol.2009.08.038.
- [4] F. De Cicco, P. Russo, E. Reverchon, C.A. García-González, R.P. Aquino, P. Del Gaudio, Prilling and supercritical drying: A successful duo to produce core-shell polysaccharide aerogel beads for wound healing, *Carbohydr. Polym.* 147 (2016) 482–489.
- [5] L.M. Comin, F. Temelli, M.D.A. Saldaña, Barley β -glucan aerogels as a carrier for flax oil via supercritical CO₂, *J. Food Eng.* 111 (2012) 625–631. doi:10.1016/j.jfoodeng.2012.03.005.
- [6] D.D. Lovskaya, A.E. Lebedev, N.V. Menshutina, Aerogels as drug delivery systems: In vitro and in vivo evaluations, *J. Supercrit. Fluids.* 106 (2015) 115–121. doi:10.1016/j.supflu.2015.07.011.
- [7] G. Tkalec, Ž. Knez, Z. Novak, Fast production of high-methoxyl pectin aerogels for enhancing the bioavailability of low-soluble drugs, *J. Supercrit. Fluids.* 106 (2015) 16–22. doi:10.1016/j.supflu.2015.06.009.
- [8] S. Quraishi, M. Martins, A.A. Barros, P. Gurikov, S.P. Raman, I. Smirnova, A.R.C. Duarte, R.L. Reis, Novel non-cytotoxic alginate–lignin hybrid aerogels as scaffolds for tissue engineering, *J. Supercrit. Fluids.* 105 (2015) 1–8. doi:10.1016/j.supflu.2014.12.026.
- [9] M. Martins, A.A. Barros, S. Quraishi, P. Gurikov, S.P. Raman, I. Smirnova, A.R.C. Duarte, R.L. Reis, Preparation of macroporous alginate-based aerogels for biomedical applications, *J. Supercrit. Fluids.* 106 (2015) 152–159. doi:10.1016/j.supflu.2015.05.010.
- [10] G. Horvat, K. Khanari, M. Finšgar, L. Gradišnik, U. Maver, Ž. Knez, Z. Novak, Novel ethanol-induced pectin-xanthan aerogel coatings for orthopedic applications., *Carbohydr. Polym.* 166 (2017) 365–376. doi:10.1016/j.carbpol.2017.03.008.
- [11] L. Goimil, M.E.M. Braga, A.M.A. Dias, J.L. Gómez-Amoza, A. Concheiro, C. Alvarez-Lorenzo, H.C. de Sousa, C.A. García-González, Supercritical processing of starch aerogels and aerogel-loaded poly(ϵ -caprolactone) scaffolds for sustained release of ketoprofen for bone regeneration, *J. CO₂ Util.* 18 (2017) 237–249. doi:10.1016/j.jcou.2017.01.028.
- [12] S. Groult, T. Budtova, Thermal conductivity/structure correlations in thermal super-insulating pectin aerogels, *Carbohydr. Polym.* 196 (2018) 73–81. doi:10.1016/j.carbpol.2018.05.026.
- [13] C.A. García-González, M. Alnaief, I. Smirnova, Polysaccharide-based aerogels—Promising biodegradable carriers for drug delivery systems, *Carbohydr. Polym.* 86 (2011) 1425–1438. doi:10.1016/j.carbpol.2011.06.066.
- [14] I. Smirnova, S. Suttiruengwong, M. Seiler, W. Arlt, Dissolution rate enhancement by adsorption of poorly soluble drugs on hydrophilic silica aerogels, *Pharm. Dev. Technol.* 9 (2004) 443–452.

- [15] I. Smirnova, S. Suttiruengwong, W. Arlt, Aerogels: Tailor-made Carriers for Immediate and Prolonged Drug Release, *KONA Powder Part. J.* 23 (2005) 86–97. doi:10.14356/kona.2005012.
- [16] L. Liu, M.L. Fishman, J. Kost, K.B. Hicks, Pectin-based systems for colon-specific drug delivery via oral route, *Biomaterials.* 24 (2003) 3333–3343. doi:10.1016/S0142-9612(03)00213-8.
- [17] J. Bhandari, H. Mishra, P.K. Mishra, R. Wimmer, F.J. Ahmad, S. Talegaonkar, Cellulose nanofiber aerogel as a promising biomaterial for customized oral drug delivery, *Int. J. Nanomedicine.* 12 (2017) 2021–2031. doi:10.2147/IJN.S124318.
- [18] B.A.C. Harley, H.-D. Kim, M.H. Zaman, I.V. Yannas, D.A. Lauffenburger, L.J. Gibson, Microarchitecture of three-dimensional scaffolds influences cell migration behavior via junction interactions, *Biophys. J.* 95 (2008) 4013–4024. doi:10.1529/biophysj.107.122598.
- [19] I. Bružauskaitė, D. Bironaitė, E. Bagdonas, E. Bernotienė, Scaffolds and cells for tissue regeneration: different scaffold pore sizes—different cell effects, *Cytotechnology.* 68 (2016) 355–369. doi:10.1007/s10616-015-9895-4.
- [20] D. Oakenfull, A. Scott, Hydrophobic Interaction in the Gelation of High Methoxyl Pectins, *J. Food Sci.* 49 (1984) 1093–1098. doi:10.1111/j.1365-2621.1984.tb10401.x.
- [21] M.L. Fishman, P.H. Cooke, H.K. Chau, D.R. Coffin, A.T. Hotchkiss, Global Structures of High Methoxyl Pectin from Solution and in Gels, *Biomacromolecules.* 8 (2007) 573–578. doi:10.1021/bm0607729.
- [22] G.T. Grant, E.R. Morris, D.A. Rees, P.J.C. Smith, D. Thom, Biological interactions between polysaccharides and divalent cations: The egg-box model, *FEBS Lett.* 32 (1973) 195–198. doi:10.1016/0014-5793(73)80770-7.
- [23] C.M.G.C. Renard, J.-F. Thibault, Degradation of pectins in alkaline conditions: kinetics of demethylation, *Carbohydr. Res.* 286 (1996) 139–150. doi:10.1016/0008-6215(96)00056-0.
- [24] S.M. Krall, R.F. McFeeters, Pectin Hydrolysis: Effect of Temperature, Degree of Methylation, pH, and Calcium on Hydrolysis Rates, *J. Agric. Food Chem.* 46 (1998) 1311–1315. doi:10.1021/jf970473y.
- [25] I. Fraeye, A. Deroeck, T. Duvetter, I. Verlent, M. Hendrickx, A. Vanloey, Influence of pectin properties and processing conditions on thermal pectin degradation, *Food Chem.* 105 (2007) 555–563. doi:10.1016/j.foodchem.2007.04.009.
- [26] L. Druel, R. Bardl, W. Vorwerg, T. Budtova, Starch Aerogels: A Member of the Family of Thermal Superinsulating Materials, *Biomacromolecules.* 18 (2017) 4232–4239. doi:10.1021/acs.biomac.7b01272.
- [27] M.A. Masuelli, Mark-Houwink Parameters for Aqueous-Soluble Polymers and Biopolymers at Various Temperatures, *J. Polym. Biopolym. Phys. Chem. J. Polym. Biopolym. Phys. Chem.* 2 (2014) 37–43. doi:10.12691/jpbpc-2-2-2.
- [28] M. Robitzer, F.D. Renzo, F. Quignard, Natural materials with high surface area. Physisorption methods for the characterization of the texture and surface of polysaccharide aerogels, *Microporous Mesoporous Mater.* 140 (2011) 9–16. doi:10.1016/j.micromeso.2010.10.006.
- [29] C. Rudaz, R. Courson, L. Bonnet, S. Calas-Etienne, H. Sallée, T. Budtova, Aeropectin: Fully Biomass-Based Mechanically Strong and Thermal Superinsulating Aerogel, *Biomacromolecules.* 15 (2014) 2188–2195. doi:10.1021/bm500345u.
- [30] C. Rudaz, Cellulose and Pectin Aerogels: Towards their nano-structuration, PhD Thesis, Ecole Nationale Supérieure des Mines de Paris, 2013. <https://pastel.archives-ouvertes.fr/pastel-00957296/document> (accessed March 7, 2018).

- [31] I.G. Plaschina, M.G. Semenova, E.E. Braudo, V.B. Tolstoguzov, Structural studies of the solutions of anionic polysaccharides. IV. Study of pectin solutions by light-scattering, *Carbohydr. Polym.* 5 (1985) 159–179. doi:10.1016/0144-8617(85)90020-7.
- [32] M.-C. Ralet, V. Dronnet, H.C. Buchholt, J.-F. Thibault, Enzymatically and chemically de-esterified lime pectins: characterisation, polyelectrolyte behaviour and calcium binding properties, *Carbohydr. Res.* 336 (2001) 117–125. doi:10.1016/S0008-6215(01)00248-8.
- [33] N. Buchtová, T. Budtova, Cellulose aero-, cryo- and xerogels: towards understanding of morphology control, *Cellulose.* 23 (2016) 2585–2595. doi:10.1007/s10570-016-0960-8.
- [34] S. Hoepfner, L. Ratke, B. Milow, Synthesis and characterisation of nanofibrillar cellulose aerogels, *Cellulose.* 15 (2008) 121–129. doi:10.1007/s10570-007-9146-8.
- [35] R. Gavillon, T. Budtova, Kinetics of cellulose regeneration from cellulose--NaOH--water gels and comparison with cellulose--N-methylmorpholine-N-oxide--water solutions, *Biomacromolecules.* 8 (2007) 424–432. doi:10.1021/bm060376q.
- [36] R. Subrahmanyam, P. Gurikov, P. Dieringer, M. Sun, I. Smirnova, On the Road to Biopolymer Aerogels—Dealing with the Solvent, *Gels.* 1 (2015) 291–313. doi:10.3390/gels1020291.
- [37] C.M. Hansen, *Hansen Solubility Parameters : A User's Handbook, Second Edition*, CRC Press, 2007. doi:10.1201/9781420006834.
- [38] J. Trygg, P. Fardim, M. Gericke, E. Mäkilä, J. Salonen, Physicochemical design of the morphology and ultrastructure of cellulose beads, *Carbohydr. Polym.* 93 (2013) 291–299. doi:10.1016/j.carbpol.2012.03.085.
- [39] C. Garnier, M.A.V. Axelos, J.-F. Thibault, Phase diagrams of pectin-calcium systems: Influence of pH, ionic strength, and temperature on the gelation of pectins with different degrees of methylation, *Carbohydr. Res.* 240 (1993) 219–232. doi:10.1016/0008-6215(93)84185-9.
- [40] F. Kar, N. Arslan, Effect of temperature and concentration on viscosity of orange peel pectin solutions and intrinsic viscosity–molecular weight relationship, *Carbohydr. Polym.* 40 (1999) 277–284. doi:10.1016/S0144-8617(99)00062-4.
- [41] F. Voragen, H. Schols, R. Visser, eds., *Advances in Pectin and Pectinase Research*, Springer Netherlands, Dordrecht, 2003. doi:10.1007/978-94-017-0331-4.
- [42] S. Paoletti, A. Cesaro, F. Delben, A. Ciana, Ionic Effects on the Conformation, Equilibrium, Properties, and Rheology of Pectate in Aqueous Solutions and Gels, in: *Chem. Funct. Pectins*, American Chemical Society, 1986: pp. 73–87. doi:10.1021/bk-1986-0310.ch007.
- [43] F. Capel, T. Nicolai, D. Durand, P. Boulenger, V. Langendorff, Calcium and acid induced gelation of (amidated) low methoxyl pectin, *Food Hydrocoll.* 20 (2006) 901–907. doi:10.1016/j.foodhyd.2005.09.004.
- [44] J.F. Thibault, M. Rinaudo, Chain association of pectic molecules during calcium-induced gelation, *Biopolymers.* 25 (1986) 455–468.
- [45] V.M. Dronnet, C.M.G.C. Renard, M.A.V. Axelos, J.-F. Thibault, Characterisation and selectivity of divalent metal ions binding by citrus and sugar-beet pectins, *Carbohydr. Polym.* 30 (1996) 253–263. doi:10.1016/S0144-8617(96)00107-5.
- [46] R. Kohn, Binding of divalent cations to oligomeric fragments of pectin, *Carbohydr. Res.* 160 (1987) 343–353. doi:10.1016/0008-6215(87)80322-1.
- [47] E.R. Morris, D.A. Powell, M.J. Gidley, D.A. Rees, Conformations and interactions of pectins: I. Polymorphism between gel and solid states of calcium polygalacturonate, *J. Mol. Biol.* 155 (1982) 507–516. doi:10.1016/0022-2836(82)90484-3.

- [48] I. Braccini, S. Pérez, Molecular Basis of Ca²⁺-Induced Gelation in Alginates and Pectins: The Egg-Box Model Revisited, *Biomacromolecules*. 2 (2001) 1089–1096. doi:10.1021/bm010008g.
- [49] P. Sriamornsak, Chemistry of pectin and its pharmaceutical uses: A review, *Silpakorn Univ. Int. J.* 3 (2003) 206–228.
- [50] C.R.F. Grosso, M.A. Rao, Dynamic rheology of structure development in low-methoxyl pectin+Ca²⁺+sugar gels1Based on a paper presented at the 3rd International Hydrocolloids Conference, 11–16 August 1996, Sydney, Australia.1, *Food Hydrocoll.* 12 (1998) 357–363. doi:10.1016/S0268-005X(98)00034-4.
- [51] C. Löfgren, P. Walkenström, A.-M. Hermansson, Microstructure and Rheological Behavior of Pure and Mixed Pectin Gels, *Biomacromolecules*. 3 (2002) 1144–1153. doi:10.1021/bm020044v.
- [52] A. Cárdenas, F.M. Goycoolea, M. Rinaudo, On the gelling behaviour of ‘nopal’ (*Opuntia ficus indica*) low methoxyl pectin, *Carbohydr. Polym.* 73 (2008) 212–222. doi:10.1016/j.carbpol.2007.11.017.
- [53] I. Fraeye, E. Doungra, T. Duvetter, P. Moldenaers, A. Van Loey, M. Hendrickx, Influence of intrinsic and extrinsic factors on rheology of pectin–calcium gels, *Food Hydrocoll.* 23 (2009) 2069–2077. doi:10.1016/j.foodhyd.2009.03.022.
- [54] M.J. Gidley, E.R. Morris, E.J. Murray, D.A. Powell, D.A. Rees, Evidence for two mechanisms of interchain association in calcium pectate gels, *Int. J. Biol. Macromol.* 2 (1980) 332–334. doi:10.1016/0141-8130(80)90060-4.
- [55] C. Garnier, M.A.V. Axelos, J.-F. Thibault, Selectivity and cooperativity in the binding of calcium ions by pectins, *Carbohydr. Res.* 256 (1994) 71–81. doi:10.1016/0008-6215(94)84228-0.
- [56] C.K. Siew, P.A. Williams, N.W.G. Young, New Insights into the Mechanism of Gelation of Alginate and Pectin: Charge Annihilation and Reversal Mechanism, *Biomacromolecules*. 6 (2005) 963–969. doi:10.1021/bm0493411.
- [57] A. Ström, E. Schuster, S.M. Goh, Rheological characterization of acid pectin samples in the absence and presence of monovalent ions, *Carbohydr. Polym.* 113 (2014) 336–343. doi:10.1016/j.carbpol.2014.06.090.
- [58] G. Agoda-Tandjawa, S. Durand, C. Gaillard, C. Garnier, J.-L. Doublier, Rheological behaviour and microstructure of microfibrillated cellulose suspensions/low-methoxyl pectin mixed systems. Effect of calcium ions, *Carbohydr. Polym.* 87 (2012) 1045–1057. doi:10.1016/j.carbpol.2011.08.021.
- [59] S.-H. Yoo, M.L. Fishman, B.J. Savary, A.T. Hotchkiss, Monovalent Salt-Induced Gelation of Enzymatically Deesterified Pectin, *J. Agric. Food Chem.* 51 (2003) 7410–7417. doi:10.1021/jf030152o.
- [60] M. A. V. Axelos, Ion complexation of biopolymers: Macromolecular structure and viscoelastic properties of gels, *Makromol. Chem. Macromol. Symp.* 39 (1990) 323–328. doi:10.1002/masy.19900390128.

Figure Captions

Figure 1

Photos of pectin aerogels from 3 wt% solutions prepared in different conditions at pH 1.5, pH 2.0 and 3.0, without the addition of salts and with addition of calcium at $R(\text{Ca}) = 0.2$. Without calcium at pH 1.5 the sample before solvent exchange was weak acid gel, at pH 2.0 it was high viscosity solution and at pH 3.0 low viscosity solutions. At $R(\text{Ca}) = 0.2$ strong ionic gels were obtained at all pH. Non-solvent was ethanol.

Figure 2

Density (a) and specific surface area (b) as a function of pectin concentration for solvent exchange performed in ethanol (open points) and acetone (filled points). Pectin was dissolved at pH 3.0, the state of the matter before solvent exchange, solution (S) or gel (G), is indicated for each case. Solid line is theoretical density for no-shrinkage case; dashed lines are given to guide the eye.

Figure 3

SEM images of pectin aerogels made from 3 wt% and 6 wt% pectin solutions at pH 3, with ethanol (a) or acetone (b) as non-solvent.

Figure 4

Viscosity as a function of shear rate of 0.9 wt% pectin solutions at different pH at 20 °C. Solid lines correspond to viscosity approximated with Cross model.

Figure 5

Zero shear rate viscosity (squares) and flow index (triangles) (see eq.4) of 0.9 wt% pectin solutions as a function of pH at 20 °C. Dashed lines are given to guide the eye.

Figure 6

Influence of pH on (a) volumetric shrinkage after solvent exchange (open points) and after sc-drying (filled points) and (b) density (open points) and specific surface area (filled points) of

pectin aerogels made from 3 wt% solutions. The state of the matter before solvent exchange is noted “G” for gel, the rest are solutions. Non-solvent used was ethanol. Dashed lines are given to guide the eye.

Figure 7

SEM images of pectin aerogel morphology made from 3 wt% solutions at different pH. The state of the matter before solvent exchange is indicated for each case. Non-solvent used was ethanol. The scale is the same for all SEM images.

Figure 8

Influence of calcium to pectin molar ratio $R(\text{Ca})$ on (a) shrinkage after solvent-exchange (open points) and after sc drying (filled points) and (b) density (open points) and specific surface area (filled points) of pectin aerogels made from 3 wt% solutions at pH 3, non-solvent was ethanol. The state of the matter before solvent exchange, solution (S) or gel (G), is indicated for each case. Lines are given to guide the eye.

Figure 9

SEM images of pectin aerogels made from 3 wt% solutions at pH 3 with calcium chloride at $R(\text{Ca}) = 0.05, 0.2$ and 0.6 . The scale is the same for all images. The state of the matter before solvent exchange is indicated for each case. Non-solvent used was ethanol.

Figure 20

Influence of sodium to pectin molar ratio $R(\text{Na})$ on (a) shrinkage after solvent exchange (open points) and after drying (filled points) and (b) density (open points) and specific surface area (filled points) of pectin aerogels made from 3 wt% solutions at pH 3, non-solvent was ethanol. The state of the matter before solvent exchange, solution (S) or gel (G), is indicated for each case. Lines are given to guide the eye.

Figure 11

(a) Density and (b) specific surface area of pectin aerogels made from 3 wt% solutions pH 3.0 with either calcium (filled symbols) or sodium (open symbols), as a function of R molar ratio. The state of matter solution (“S”) or gel (“G”) is given for each case. Dashed lines are given to guide the eye.

Figure 12

Density and specific surface area of pectin aerogel made from 3 wt% solutions, non-solvent is ethanol.

Figure 13

Schematic presentation of two main ways of structure formation, from solution to aerogel

Appendix A:

Supplementary Information

Tuning structure and properties of pectin aerogels

Sophie Groult, Tatiana Budtova*

Figure S1

Reduced viscosity of pectin solution in 0.01 M NaCl at 26.6 °C. Solid line is linear approximation. The intersection with Y axis gives intrinsic viscosity.

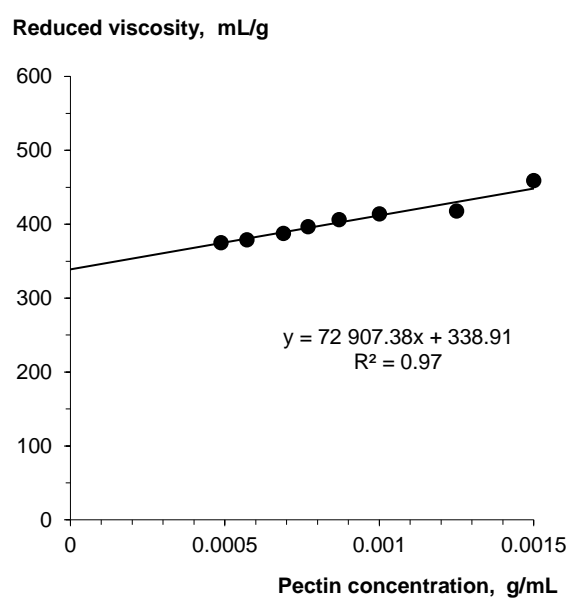


Figure S2

Volumetric shrinkage ΔV after solvent exchange (triangles) and after sc drying (circles) as a function of pectin concentration. Pectin was dissolved at pH 3; non-solvent was either ethanol (open points) or acetone (filled points). The errors are smaller or of the size of symbols. The state of matter before solvent exchange, solution (S) or gel (G), is indicated for each case. Lines are given to guide the eye.

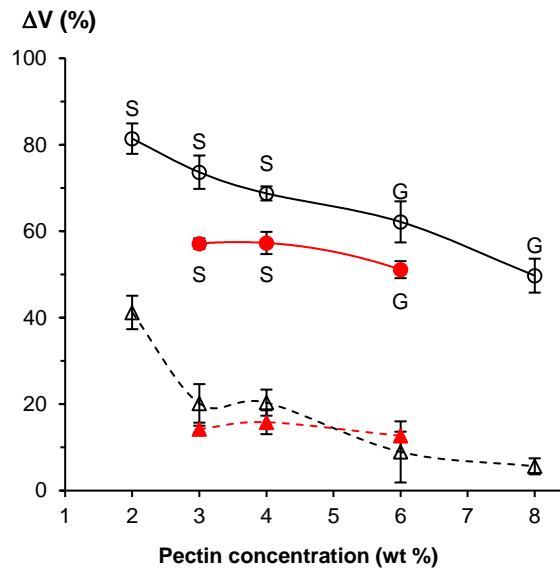


Figure S3

Comparison of (a) density and (b) specific surface area of pectin aerogels made from 3 wt% solution at pH 2 and 3, using either ethanol (open) or acetone (filled) as the non-solvent.

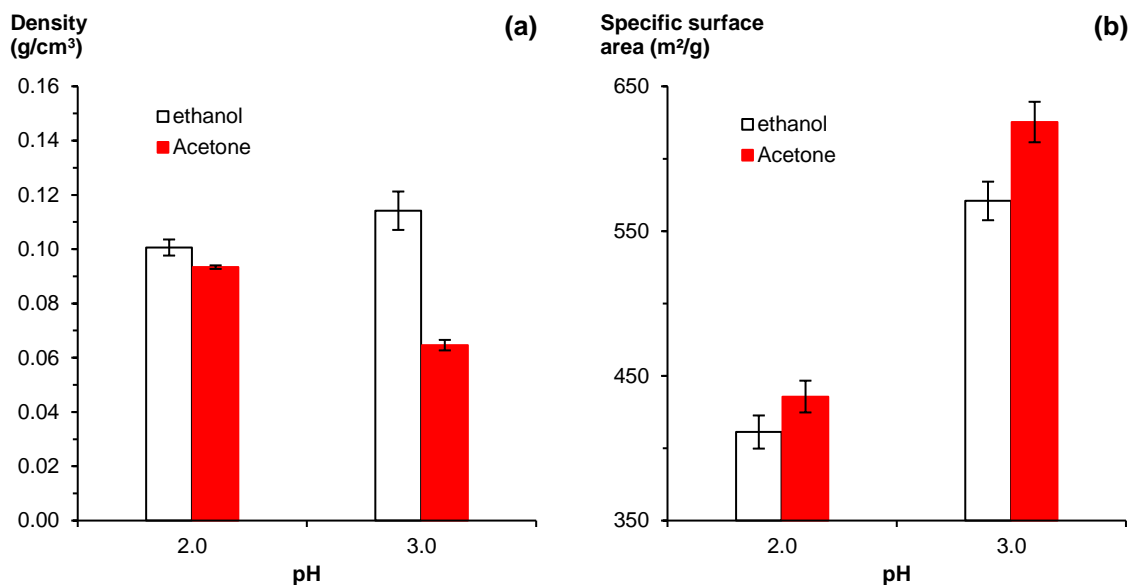


Figure S4

(a) Pectin aerogel porosity and (b) specific pore volume of the same samples as shown in Figure 2, with either ethanol (open) or acetone (filled) points as non-solvent. Lines are given to guide the eye.

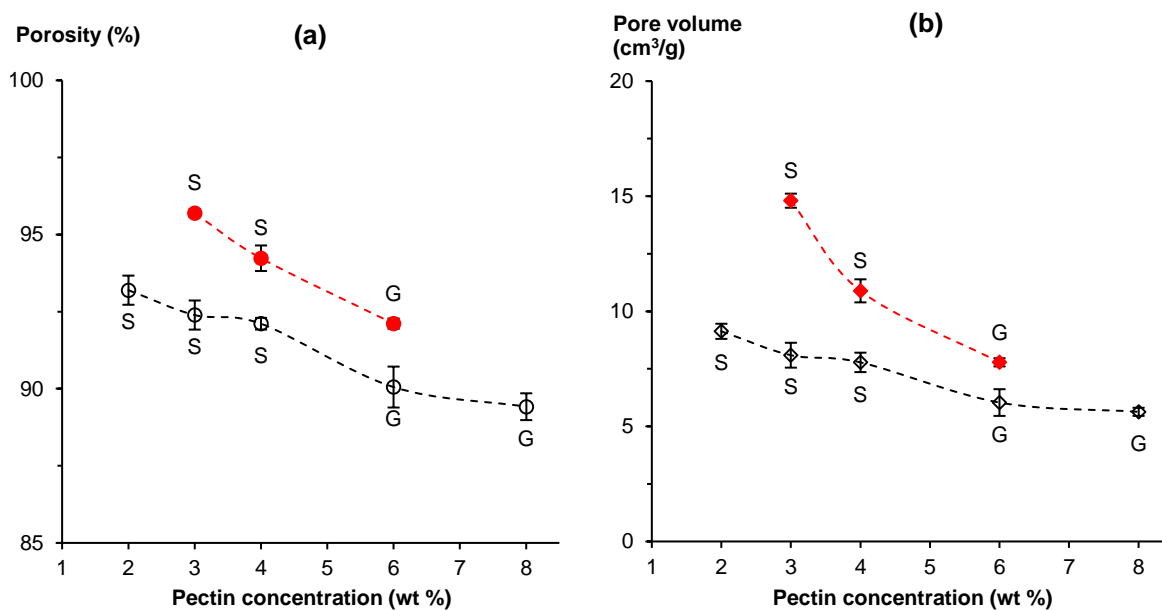


Figure S5

High magnification SEM image of pectin aerogel made from 3 wt% pectin using acetone as non-solvent. Fibril thicknesses D (in nm) were estimated using SEM software.

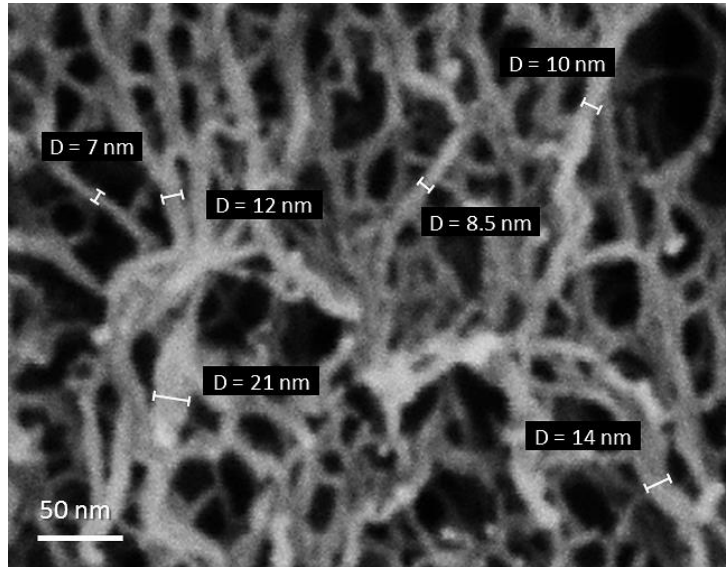


Table S1

Fitting parameters for flow curves (Figure 4) according to eq.4

pH	1.6	2	2.5	2.7	3	3.5	4	6	8
n	0.5824	0.5556	0.5562	0.5016	0.4519	0.3606	0.0116	0.0110	0.0100
η_0 (Pa s)	0.7262	0.4202	0.2240	0.0810	0.0546	0.0394	0.0226	0.0252	0.0254
α (s)	0.2507	0.1279	0.0378	0.0046	0.0012	0.0005	0.0048	0.0043	0.0046

Figure S6

(a) Porosity and (b) pore volume of pectin aerogels (same as in Figure 6) made from 3 wt% solutions at different pH, non-solvent was ethanol. The state of the matter before solvent-exchange is noted “G” for gel, the rest are solutions.

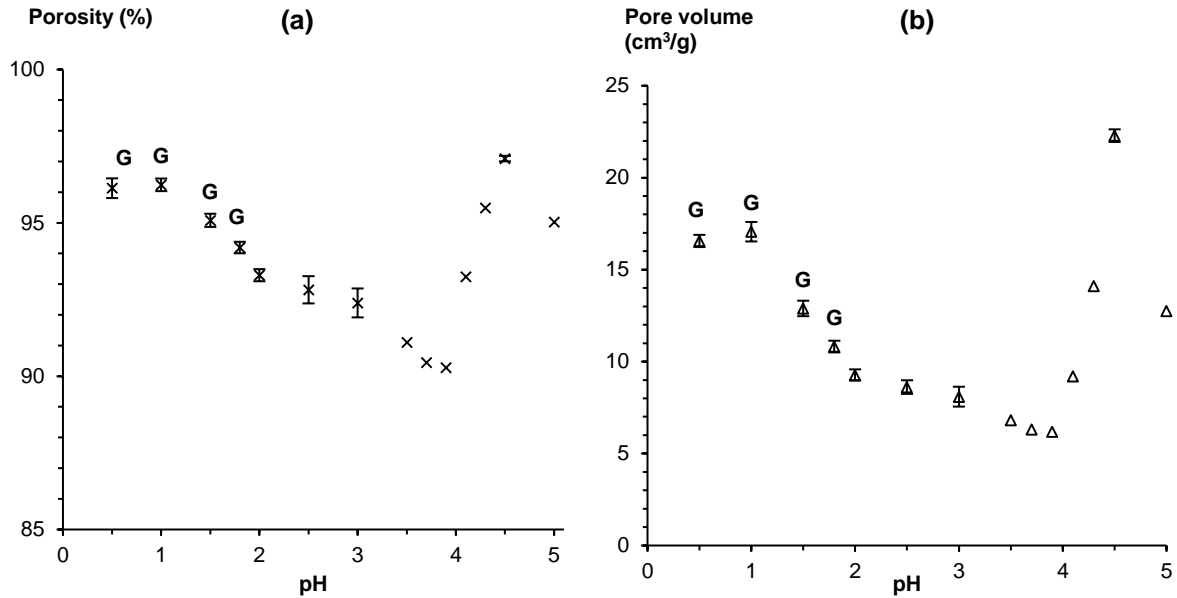


Figure S7

Pectin aerogels made from 3 wt% dissolved at pH 3, with increasing R(Ca) from 0 to 0.6, non-solvent was ethanol. The state of matter before solvent exchange, solution (S) or gel (G), is indicated for each case.

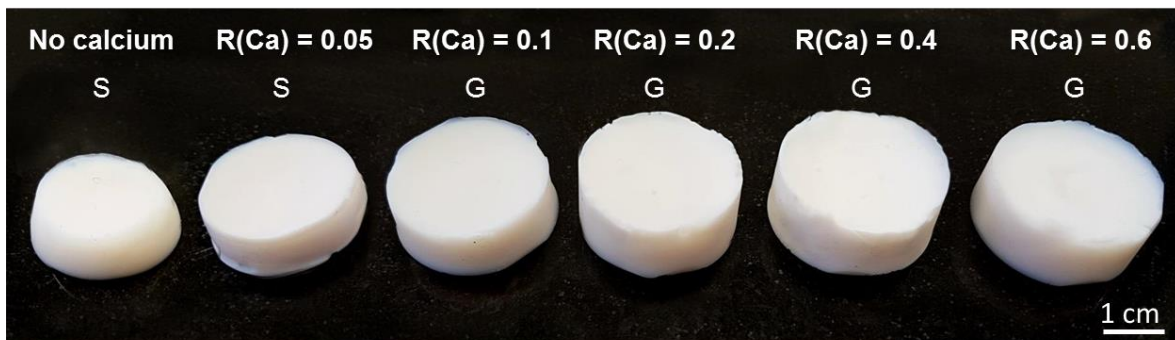


Figure S8

Influence of calcium to pectin molar ratio on (a) porosity and (b) pore volume for pectin aerogels made from 3 wt% at pH 3 (same as in Figure 8), non-solvent was ethanol. The state of matter before solvent exchange, solution (S) or gel (G), is indicated for each case.

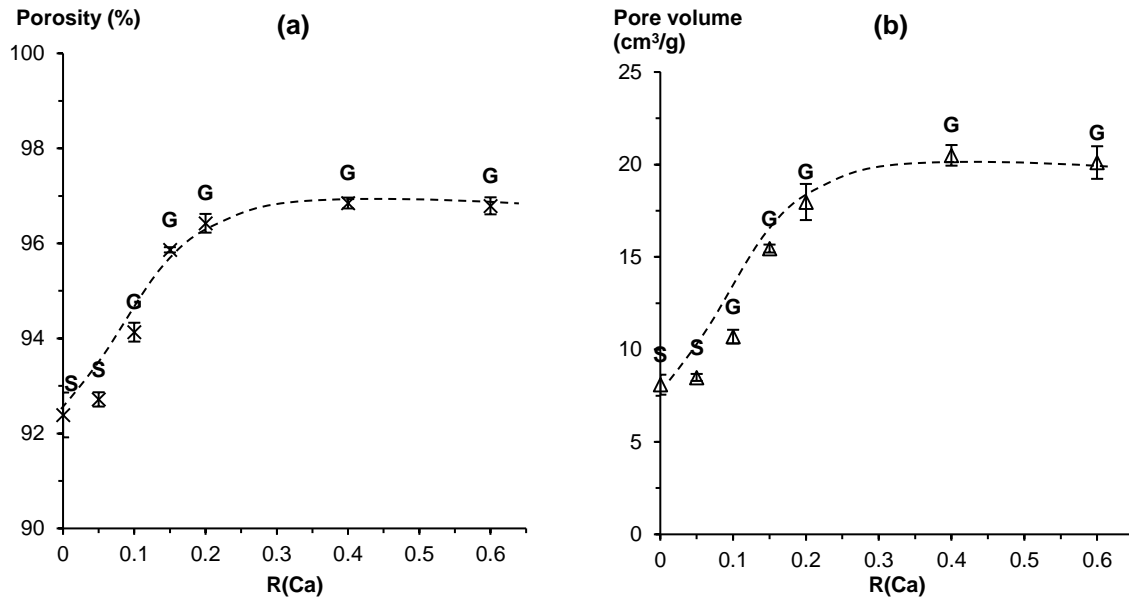


Figure S9

Density (open points) and specific surface area (filled points) of pectin aerogels made from 3 wt% solutions at pH 2 as a function of calcium to pectin molar ratio $R(\text{Ca})$. The state of the matter before solvent exchange, solution (S) or gel (G), is indicated for each case. Non-solvent was ethanol. Lines are given to guide the eye.

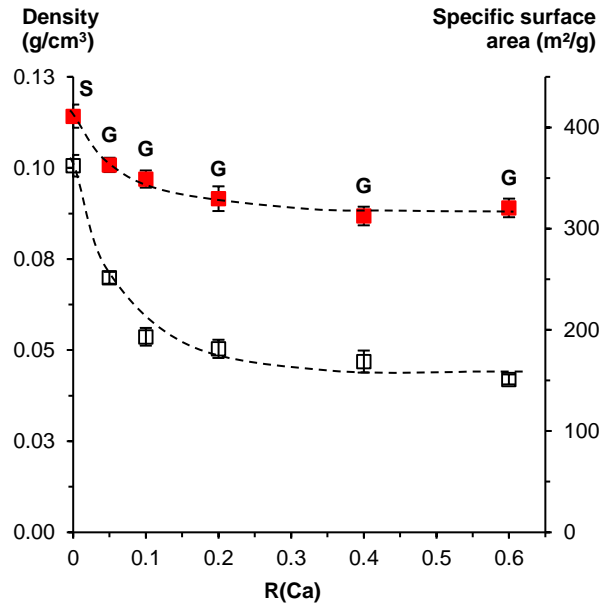


Figure S10

Photos of pectin aerogels made from 3 wt% solutions at pH 3 with different amount of NaCl added. Samples were solutions at $R(\text{Na}) = 0.2$ and strong gels at $R(\text{Na}) = 1$ and $R = 2$. Non-solvent was ethanol.

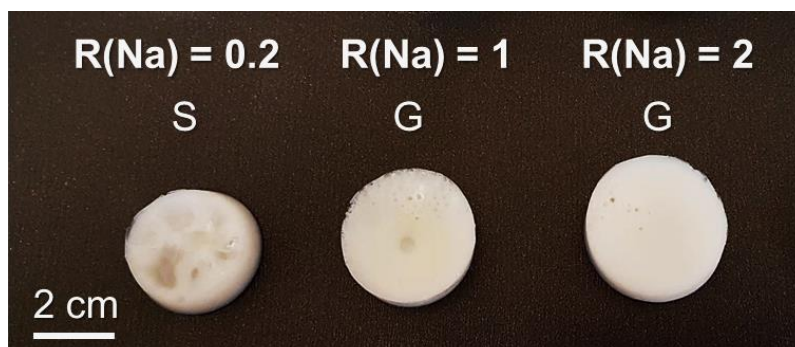


Figure S11

Influence of sodium to pectin molar ratio on (a) porosity and (b) pore volume for pectin aerogels made from 3 wt% at pH 3 (same as in Figure 10). The state of the matter before solvent exchange, solution (S) or gel (G), is indicated for each case. Non-solvent was ethanol.

Lines are given to guide the eye.

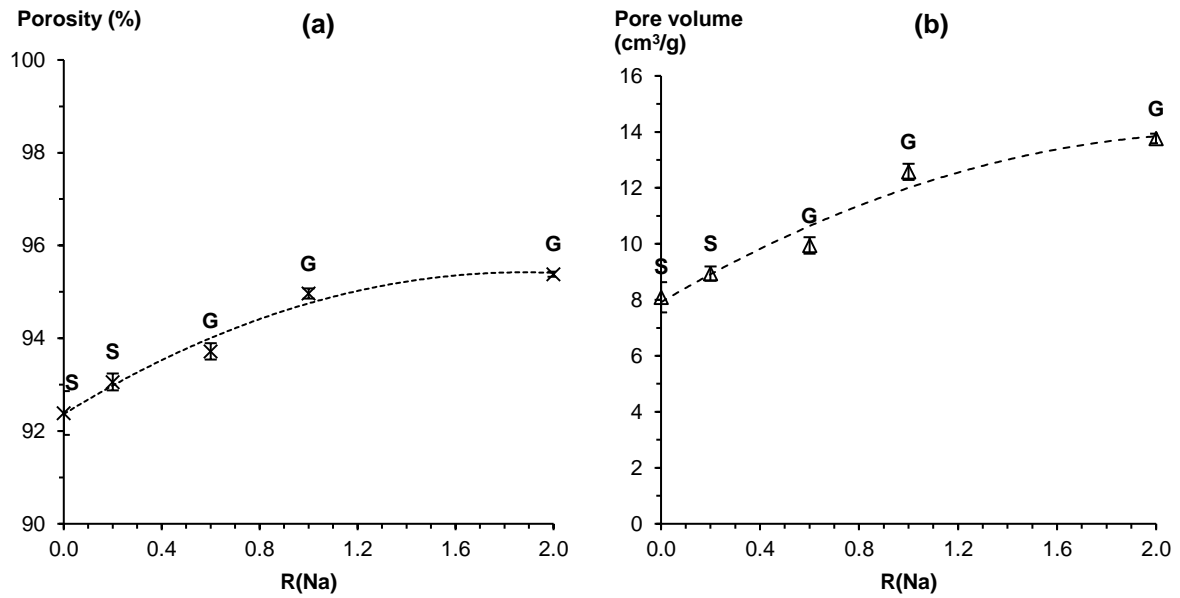


Figure S12

Influence of sodium to pectin molar ratio $R(\text{Na})$ on (a) shrinkage after solvent exchange (open points) and after drying (filled points) and (b) density (open points) and specific surface area (filled points) of pectin aerogels made from 6 wt% solutions at pH 3, non-solvent was ethanol. The state of the matter before solvent exchange, solution (S) or gel (G), is indicated for each case. Lines are given to guide the eye.

